International Journal of Engineering Trends and Technology
ISSN: 2231-5381/ https://doi.org/10.14445/22315381/IJETT-V74I11P123

Volume 74 Issue 11, 343-378, November 2026
© 2026 Seventh Sense Research Group®

Review Article

Abnormal Lubricant Film Pressure Distribution in Sliding AISI 52100 Ball Bearings: Coupled Analysis of Contact Fatigue and Wear Behaviour

Joseph O. Dirisu[1*,2], Thywill Cephas Dzogbewu[1,2], Enesi Y. Salawu[3]

[1]*Department of Mechanical and Mechatronics Engineering, Central University of Technology, Bloemfontein, Free State, South Africa.*
[2]*Centre for Rapid Prototyping and Manufacturing, Central University of Technology, Bloemfontein, Free State, South Africa.*
[3]*Department of Mechanical Engineering, Wigwe, Isiokpo, Rivers State, Nigeria.*

[*]*Corresponding Author: jdirisu@cut.ac.za*

Received: 07 February 2026 Revised: 30 July 2026 Accepted: 30 September 2026 Published: 25 November 2026

Abstract *- The disruption of standard Hertz/ Elastohydrodynamic Lubrication (EHL) predictions by roughness-induced micro-contacts, inlet starvation, shear-thermal effects, and third-body debris lead to abnormal pressure distributions in lubricated point contacts under pure sliding. Because of the implications for fatigue start and wear development in bearing steels, there has been an increasing interest in characterizing anomalous lubricant film pressure distributions in rolling-sliding and pure sliding contacts. A representative platform for analyzing the relationship between wear behaviour, sliding contact fatigue, and lubrication mechanics is offered by AISI 52100 ball bearing contacts. This paper summarizes what is now known about the causes and development of non-classical pressure distributions under pure sliding, considering the impact of surface roughness, subsurface stress fields, and lubricant rheology. The connection between tribo-oxidation, stress concentration events, and microstructural alterations that lead to localized deviations from Hertzian theory is highlighted. Along with experimental methods like fatigue mapping, in-situ imaging, and high-resolution layer thickness measurement, the research also discusses modeling approaches that integrate tribochemistry with elastohydrodynamic and mixed lubrication frameworks. A rigorous analysis shows how abnormal pressure profiles accelerate bearing failure, spread wear scars, and accelerate the beginning of cracks. The review concluded by making recommendations for future research, including multiscale modeling of tribo-chemical-mechanical interactions, advanced in-situ diagnostics, and the development of predictive design tools for lubricant and bearing material optimization.*

Keywords *- AISI 52100, Abnormal lubricant, Bearing failure, Elastohydrodynamic, Stress concentration.*

1. Introduction

Lubrication is a major issue that is of great importance in process industries, and one of the most important tasks that maintenance engineers are required to perform is the choice of the lubricant, as well as the appropriate combination of performance-enhancing additives [1-3]. Lubricants play the role of the heart of machine since they are responsible in minimizing friction between moving surfaces and excessive degradation of the parts [4, 5].

Industrial lubricants based on mineral oils of fossil occurrence are the most used, and their tribological behaviour has been extensively studied [6-9]. Most literature advises adding components to enhance performance, and commercial formulations normally have 90-95% of base oil and 5-10% of additives [10-12]. With the ever-increase in the demand of high-performance lubricants, the focus has now been on solid lubricant additives like Tungsten Disulphide (WS_2) and Molybdenum Disulphide (MoS_2), which are known to be efficient emergency extreme-lubricants [13, 14]. The capability of MoS_2 and other sulphide-based compounds to form stable boundary films is one of the primary attributes in the minimization of friction and wear [15, 16]. Previous studies also reveal that the smaller the size of MoS_2 particles, the better the tribological characteristics [17-21]. Similarly, submicron hydrophobic MoS_2 particles in Poly-Alpha-Olefin (PAO) oils have shown ultra-low coefficients of friction (0.02), and the role of appropriate dispersants [22].

Additive morphology is also an important consideration in the performance; Molybdenum Dithiocarbamate (MoDTC) dispersed in low-viscosity oils improves lubrication by first breaking down to MoS_2 [23-26]. Equally, tungsten disulphide has demonstrated great potential in application as a lubricant

This is an open access article under the CC BY-NC-ND license (http://creativecommons.org/licenses/by-nc-nd/4.0/)

additive, with multiple studies reporting better friction and wear behaviour with the addition of lamellar WS_2 or MoS_2 structures into an oil-based lubricant [27-30]. The lamellar structure of rare-earth-based additives in layered form is largely seen as one of the key attributes that make them so highly tribological.

In the paper of Bhaumik [31], the mineral oils were improved with the additives of WS_2, MoS_2 and lithium Potassium Titanate (PT) by means of four-ball tribometer. The level of minimum friction was reached when 3 wt.% PT, MoS_2, and 2 wt.% WS_2 were used, and WS_2 produced the least total friction coefficient. Nevertheless, PT generated the values of smallest wear scars, followed by MoS_2, which indicates high-quality anti-wear performance. Microscopy revealed that PT-blended oil resulted into slight damage to the surface in contrast to other additives. All additive-enriched oils were found to be similar in the extreme-pressure tests, and none of them welded at 1260 N, as did the base oil, which welded at that load-carrying capacity, showing an improvement of the load-carrying capacity.

PT-added oil recorded the highest fatigue life in rolling-contact fatigue tests, followed by the MoS_2 and the WS_2, indicating that PT can be used as an alternative to traditional solid lubricants. The results of the research have shown that the tribological life of AISI 52100 bearing steel is remarkably enhanced by the inclusion of appropriate additives [32]. Jain [33] states that rolling bearings are supposed to be functioning even in the conditions of the severe working conditions, which is why their internal design is a crucial factor of the overall performance.

Each part of a bearing must be streamlined to obtain the required reliability of operations and ability to carry a load. Many factors affect the service life of bearing, the material properties, contact geometry, quality of lubrication, operating loads and environmental conditions being a few. Therefore, a large amount of literature has been devoted to the lengthening of bearing life by improving heat treatment operations, superior surface finishes, and ideal surface roughness. Concurrently, a great deal of focus has been placed on improving bearing design using simulation methods based on finite elements that enable precise prediction of stress distribution, deformation, contact relations, and the start of failure.

All of this has contributed to the development of more reliable and efficient rolling bearings that can be used in modern industrial operations. Jain [33] states that wear resulting from sliding contacts between the big end of the roller and the cone flange surface is what causes the loss of preload in tapered roller bearings. They discover that wear is minimized in the region of 0.04 to 0.10 μm on the disc surface under test conditions. To reduce wear during the bearing run-in stage, it is advantageous to keep the cone's flange roughness within this range. After the final grinding procedure, additional honing or superfinishing can achieve this ideal roughness (R_a = 0.04-0.10 μm).

The performance and dependability of ball bearings are largely dependent on the stability of the lubrication film and formation in the rolling-sliding contact zone. In an ideal Elastohydrodynamic Lubrication (EHL) scenario, the lubricant film's pressure field is symmetric and smooth, minimizing surface distress and providing sufficient space between the interacting surfaces. However, the lubricant film may generate aberrant pressure distributions under practical working situations, such as high load, temporary start-up/shut-down, contamination, misalignment, and localized temperature rise [31].

These include film collapse regions, local spikes, distorted pressure peaks, and micro-pitting-related distortions. In AISI 52100 steel ball bearings, a common bearing material because of its high hardness, fatigue resistance, and predictable microstructural response, such non-classical EHL behavioural characteristics become crucial. The defects in the sphere of lubricant pressure can accelerate the process of fatigue and wear. The concentration of subsurface stress is an encouragement to micro-cracking and premature Rolling Contact Fatigue (RCF).

Simultaneously, film thinning also improves asperity contacts that augments adhesive and abrasive wear. With time, these synergistic processes eroded bearing geometry, distorted the surface roughness and caused additional disturbed lubrication regime in a self-perpetuating process of early failure. Despite all the efforts made in the modelling of EHL, the coupled analysis that would incorporate the representations of the anomalies of lubricant pressure with real wear development and the trend of the fatigue initiation [31] will be necessary.

Recent literature has been growing less concerned with pressure distribution, wear development, and fatigue behaviour, but they are considered separately. This leads to the fact that the combined effect of non-Hertzian pressure anomalies on fatigue-wear interaction has not been addressed adequately.

Although there is a lot of research on lubricant additives and classical Elastohydrodynamic Lubrication (EHL) behaviour, most studies assume ideal pressure distributions and do not adequately consider any abnormal pressure phenomena occurring under realistic operating conditions, such as high loads, sliding contacts and transient regimes. Furthermore, most of the literature treats wear, fatigue, and lubrication behavior as separate problems; the coupled behavior of wear, fatigue, and lubrication behavior has not received much attention.

It is unclear how non-classical lubricant pressure distributions affect the development of subsurface stress, the start of cracks, and the advancement of wear in AISI 52100 bearing steels. The problem of accurately predicting premature bearing failure in practice services in practical service conditions is hampered by this gap.

This work develops an integrated framework that combines Elastohydrodynamic Lubrication (EHL) behavior, finite element stress analysis, and experimental data to investigate how aberrant lubricant film pressure distributions impact the coupled evolution of wear and rolling contact fatigue in AISI 52100 bearing steel. In contrast to earlier research that typically treats lubrication behavior, wear, and fatigue as separate or weakly coupled phenomena, this work specifically identifies and analyzes the role of non-Hertzian pressure anomalies as a driving mechanism for lubrication regime transition, subsurface stress intensification, and fatigue crack initiation. The impact of pressure irregularities is further isolated by focusing on pure sliding situations, providing a better mechanistic explanation of failure progression under less-than-ideal operating conditions.

This study uses AISI 52100 ball bearings to investigate the anomalous distribution of lubricant film pressure in sliding contacts and how it affects wear and fatigue behavior. The formation of pressure irregularities, their effects on subsurface stress fields, and the ensuing mechanisms of material removal and crack initiation are all examined in this paper. Finite element stress analysis, EHL lubrication models, and experimentally recorded wear and Rolling Contact Fatigue (RCF) data are used in an integrated way to achieve this.

In order to shed light on how variations from classical elastohydrodynamic behavior contribute to surface damage and fatigue degradation in AISI 52100 bearing contacts, the work specifically focuses on abnormal lubricant film pressure distributions under pure sliding conditions and their coupling with sliding-contact fatigue and wear processes.

2. Contact Pressure Distribution and Lubrication Effects on AISI 52100 Bearing Steel

Contact-pressure distribution is a key idea in the field of friction and wear engineering because it controls the mechanical and tribological behavior of interfaces between high-concentration point contacts (in rolling-element bearings) or distributed area contacts (in seals), according to Stachowiak and Batchelor [34].

Contact geometry, material properties, surface roughness, and applied load all have a significant impact on the pressure distribution. Designing mechanical systems that are more robust, efficient, and long-lasting will be made possible by a thorough understanding of the evolution of the pressure distribution.

Hertzian contact theory, which provides analytical solutions for contact stresses and elastic deformations of normal loading, is frequently used to describe pressure and stress fields in the situation of smooth elastic bodies [35]. Nevertheless, in most practical tribological contacts, there is a deviation of Hertzian assumptions because of the existence of adhesion, plastic deformation, surface roughness or effects caused by sliding. Pressure distribution in lubricated contacts is another, more important parameter: this determines the entrainment of lubricants, the growth of film thickness, frictional behaviour, and the wear and fatigue behaviour in the end.

In hydrodynamic and Elastohydrodynamic Lubrication (EHL), load-carrying capacity and separation of surfaces are directly dependent on the pressure distribution in the movement of the lubricant film [36, 37]. High pressure in the contact enhances the density and viscosity of lubricants and facilitates the development of a load-bearing film which eliminates direct asperity contact at high loads.

Local film thickness, friction and changing between full-film, mixed and boundary lubrication regimes are therefore governed by the shape of the pressure profile [38]. Non-uniform or non-optimal pressure distributions, e.g. loading at the edges, spiked pressures, etc., may cause high subsurface stress, enhance surface fatigue, and facilitate a range of damage mechanisms including micropitting, spalling, and the formation of cracks.

The thermal and dynamic behaviour of lubricated contacts is also dependent on the pressure distribution. Viscous shear heating caused by high local pressures may destabilize the lubricant by oxidation, loss of viscosity, or breaking of the film. Imbalanced pressure distribution in rotating equipment can also cause vibration, noise, and instability in operation, especially in rolling element bearings.

Therefore, precise prediction and control of pressure fields through analytical models, numerical computations or experimental results are needed to optimize component design, lubrication choice, working condition, and service life [39, 40]. These effects are of special significance to AISI 52100 bearing steel, 100Cr6, or AISI 52100 bearing steel which is among the most widely studied materials in the field of tribology and bearing engineering [41].

After proper heat treatment, AISI 52100 attains hardness levels of around 60-66 HRC, which offer tremendous resistance to plastic deformation and abrasive wear both under rolling and sliding and contact conditions.

A fine martensitic microstructure with dispersed carbides gives it excellent Rolling Contact Fatigue (RCF) resistance and is a reference material to fatigue life experiments and to assess the fatigue life of new alloys, surface treatments and

lubrication methods. AISI 52100 is highly sensitive to lubrication conditions because to its widespread use and favourable mechanical characteristics.

This steel is commonly used to create bearings that function at Hertzian contact pressures of 1-4 GPa, where even a small rupture in the lubricant layer can cause asperity contact and rapid surface damage [42].

Under mixed or boundary lubrication, localized stress concentration, frictional heating, and tribo-oxidation may promote the formation of cracks, micropitting, and spalling. Additionally, AISI 51200 has a lower inherent corrosion resistance than stainless bearing steels and is more vulnerable to corrosion-fatigue interactions, tribo-oxidative layers, and white etching fractures in poor lubrication, contamination, or sliding conditions [43].

Because of these features, AISI 52100 is a perfect model material for examining lubricant film pressure inconsistencies and how they relate to wear and fatigue processes. Its extensive historical database, industrial relevance, and well-documented failure modes provide a robust foundation for studying how deviations from classical elastohydrodynamic behaviour accelerate damage in rolling and sliding bearing contacts.

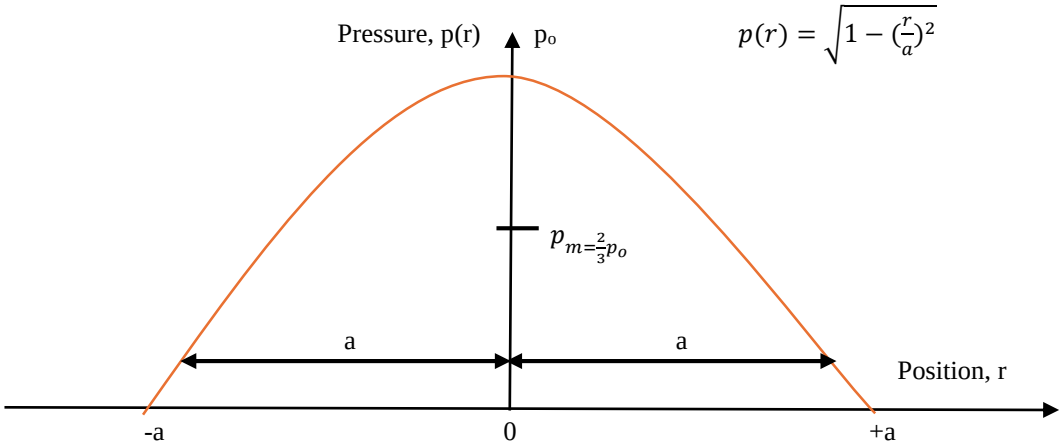

Fig. 1 Classic dome / parabola hertzian pressure distribution [44]

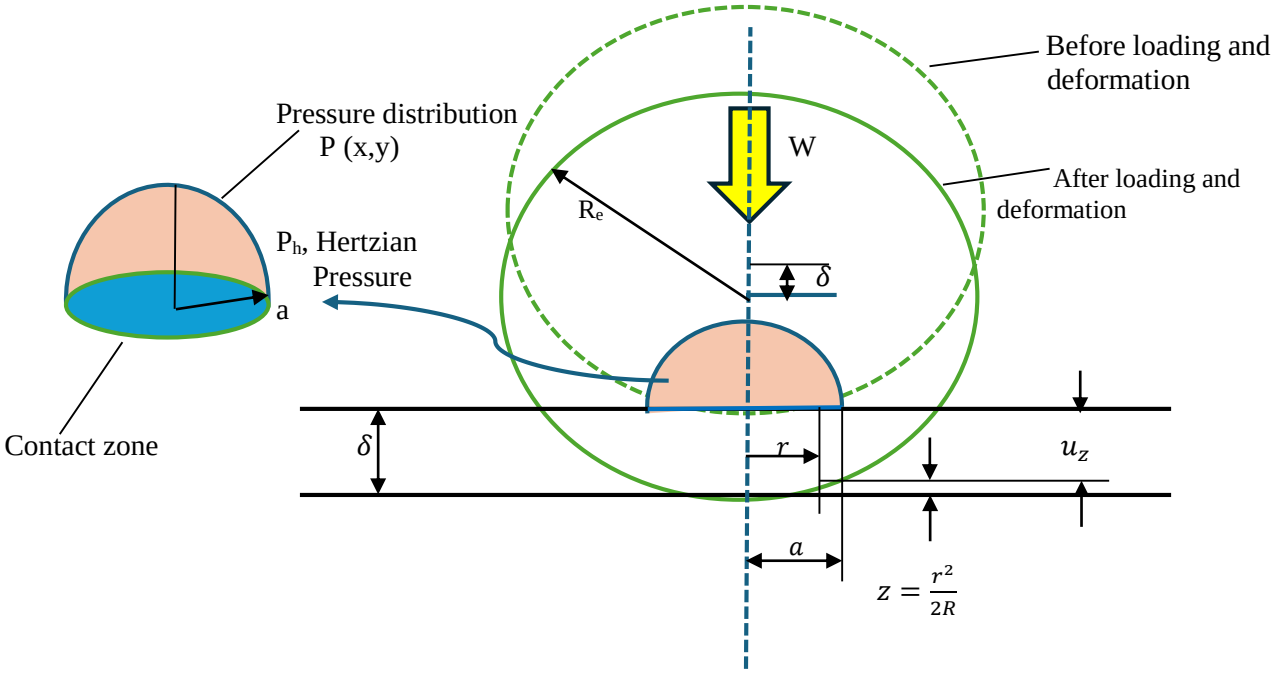

Fig. 2 Presents hertz contact geometry and contact $p(r) = po\sqrt{(1 - (\frac{r}{a})^2)}$ [44]

Figure 1 Shows the classic dome / parabola Hertzian pressure distribution (Ideal point/elliptical contact) with pressure = 0 at the contact edge. Figure 2 presents Hertz contact geometry and contact $p(r) = po\sqrt{(1} - (\frac{r}{a})^2)$patch illustration (sphere/half-space).

Schematic of a sphere on a flat (or two spheres), defining contact radius a, approach, and the elastic half-space assumptions used by Hertz. Useful for deriving a

$$a = \frac{3WR}{4E^*}^{\frac{1}{3}} \quad (1)$$

2.1. Elastohydrodynamic and Mixed Lubrication in Concentrated Bearing Contacts

In many machine-element interactions, loads are transmitted through thin, continuous lubricant films that separate opposing surfaces. Experimental evidence has long confirmed the validity of classical hydrodynamic lubrication theory for conformal contacts such as journal and thrust bearings.

However, for highly loaded contacts with limited geometric conformity such as rolling-element bearings and gears early hydrodynamic theories failed to adequately predict observed behaviour. Discrepancy arose because these models neglected elastic deformation of the contacting surfaces under high contact pressures.

The integration of hydrodynamic lubrication theory with elastic contact mechanics led to the development of Elastohydrodynamic Lubrication (EHL), which provides a more accurate description of lubrication in such concentrated contacts. In EHL, the lubricant experiences extreme pressures that significantly increase its viscosity, while elastic deformation of the contact surfaces enlarges the contact area and facilitates film formation.

The Reynolds equation and the elastic deformation equations must be solved simultaneously to perform an accurate EHL analysis [44]. Elastohydrodynamic lubrication is suitable for highly compliant systems like elastomeric bearings, seals, and even biological joints, and it regulates the performance of crucial, heavily loaded parts like gears, rolling-element bearings, cams, and followers [45].

Most classic EHL evaluations have focused on pure rolling situations, where the direction of lubricant entrainment coincides with the minor axis of the Hertzian contact ellipse. Even though this assumption is adequate for many applications, it does not adequately account for the range of contact configurations observed in practice.

For example, in high-conformity gearing and roller-rib contacts of cylindrical and tapered roller bearings, the lubricant entrainment vector may be parallel to the major axis of the contact ellipse, resulting in basically differing pressure and film-thickness distributions [46].

These flow-direction effects are especially important in sliding or mixed rolling-slide conditions, where deviations from typical EHL behavior may arise. Over the past 20 years, a great deal about mixed EHL occurs, a regime where intermittent asperity contact coexists with hydrodynamic film production.

Since most power-transmitting components function in this regime and full-film lubrication and dry contact are limiting instances of the same physical framework, mixed EHL is practically significant. Recent unified mixed-lubrication models now incorporate contact mechanics, hydrodynamic lubrication, and surface roughness within a single mathematical formulation, enabling simulation of the full transition from full-film lubrication through mixed lubrication to boundary or dry contact [47].

These developments have successfully achieved a bridge between two traditionally distinct fields of contact mechanics and lubrication theory, resulting in a wider view of interfacial mechanics, which combines mechanical, chemical, and physical interactions at tribological interfaces.

The micro-Elastohydrodynamic Lubrication (micro-EHL) is an extension of the EHL ideas whereby the roughness on the surfaces is considered at smaller dimensions. Dawson and Jin studies [48] established that micro-EHL is playing great role in the development of effective lubricating films in synovial joints and other compliant contacts.

Their results indicated that the amplitude of roughness and wavelength have a high impact on minimum film thickness and no effect on phase angle. Despite the reduction in film thickness by short wavelength and high amplitude roughness, micro-EHL was observed to be an effective means of lubrication over a large variety of conditions. The paper was also able to note the effect of conjunction kinematics between pure rolling and sliding on the development of films.

The progress of experiments has played a pivotal role in the process of justifying and perfecting EHL and mixed-EHL theories. Spikes [49] offer a detailed description of the experimental methods employed in the study of elastohydrodynamic lubrication and they include ultra-thin film interferometry, fluorescence spectroscopy, in-contact infrared and Raman spectroscopy, temperature and shear-stress mapping, and measuring the film-thickness methods.

These methods have greatly improved our knowledge of lubricant stability, lubricant breakdown, and film production in EHL-all of which strongly rely on real-world observation for the interpretation and development of theoretical models.

In Hertzian Contact Theory, a dry elastic contact (i.e. no lubricant) will assume a parabolic form whenever two elastic bodies (e.g. ball on a flat, roller on a raceway, etc.) are put under compression. For a circular (point) contact:

$$p(r) = po\sqrt{(1 - (\frac{r}{a})^2)}, 0 \leq r \leq a \quad (2)$$

Po is the maximum pressure at the centre of contact, and pressure gradually decreases toward the edges until it reaches zero at the contact boundary. It has a dome-like curve that resembles a paraboloid. This normal prediction is characterized by a smooth, symmetrical parabola-shaped pressure distribution with a maximum in the centre and zero at the edges.

The normal pressure and lubricant film distributions inside a concentrated contact under isothermal Elastohydrodynamic Lubrication (EHL) conditions are significantly different from what classical Hertzian contact theory predicts. In dry Hertzian contact, the pressure distribution is characterized by a smooth parabolic profile with a maximum at the centre of the contact and zero pressure at the edges, with load supported solely by elastic deformation of the contacting bodies.

On the other hand, the coupled action of hydrodynamic effects and elastic deformation controlled by the Reynolds equation modifies the pressure distribution when a lubricant is entrained into contact.

The hydrodynamic wedge effect, which pulls the lubricant into the conjunction, causes the lumbar pressure to gradually rise in the inlet area of a typical contact EHL contact. Both pressurized lubricating film and elastic deformation sustain the applied load, as evidenced by the pressure distribution in the central contact zone, which is practically flat-headed and still resembles a Hertzian plateau.

A sharp pressure spike appears near the exit (trailing edge) of the contact with lubricant squeezed and forced to discharge through the reduced gap. This spike in the exit pressure is an indicative attribute of EHL contacts and one of the greatest deviations of classical Hertzian behaviour.

This pressure development is reflected in the shape of the lubricant film that results. The movie gradually collides at the inlet area to create a wedge shape profile which favours the formation of hydrodynamic films. The film is relatively thick and flat at the central point of contact, which provides the support to the applied weight.

As one moves towards the outlet, the film thickness reduces very quickly, and the film attains a minimum near the trailing edge. The classical EHL theory thus forecasts the occurrence of a wedge-shaped or horseshoe film profile with a flat central region and the minimum film thickness at the exit.

The HamrockDowson equations are widely used as equations of central film thickness (h_o) and minimum film thickness (h_m) under EHL conditions to obtain quantitative predictions that are often used in the analysis and design of engineering systems [50].

The isothermal EHL pressure field according to Habchi et al. [51] can be considered as the combination of a Hertz-like central plateau of pressure and an exit pressure spike, and the thickness profile of the film shows a flat central plateau and a significant minimum in the rear area.

Such pressure and film shapes are normally said to show a stable or healthy elastohydrodynamic lubrication. This classical behaviour may be perturbed by non-classical behaviour, e.g. distorted pressure profiles, multiple pressure spikes, non-uniform film shapes or film rupture, which is usually linked to abnormal lubrication conditions, e.g. starvation, contamination, excessive sliding, or the early onset of surface damage and wear.

The variation of pressure and film morphology are, hence, good diagnostic measures of lubrication performance and impending failure of rolling and sliding bearing contacts.

3. Review Methodology and Analytical Framework

This study adopts an integrated methodological framework that combines theoretical Elastohydrodynamic Lubrication (EHL) modelling, Finite Element Analysis (FEA), and experimental evidence from the literature to investigate the coupled effects of abnormal lubricant film pressure distributions on wear and Rolling Contact Fatigue (RCF) in AISI 52100 bearing steel.

The objective is to establish a mechanistic link between lubrication behaviour, pressure distribution, and material response under non-ideal operating conditions.

The overall workflow of the approach is illustrated in Figure 3.

The key justifications of the approach in Figure 3 are as follows:

1. Pure sliding isolates the effect of pressure anomalies.
2. Linear elastic assumption valid for bearing steels under contact (small strains).
3. Steady-state EHL appropriate for contact speed and load.
4. Boundary conditions represent actual test conditions.
5. Model validated at each stage with available data.

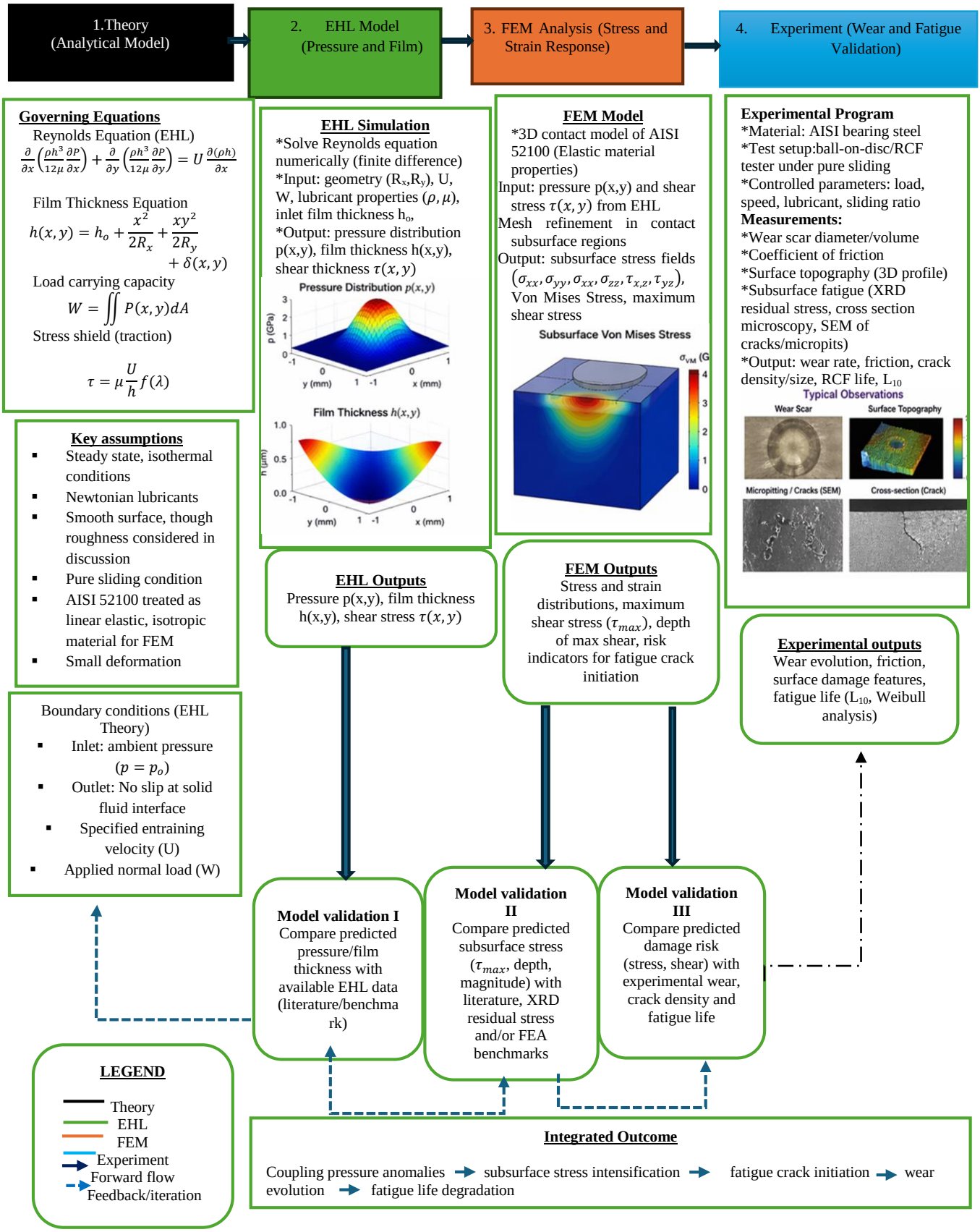

Fig. 3 Workflow illustrating the coupling between lubrication modelling, stress analysis, and experimental evidence

3.1. Theoretical Framework: Elastohydrodynamic Lubrication (EHL)

The lubrication behaviour in concentrated contacts is described using classical elastohydrodynamic lubrication theory, in which the pressure distribution and film thickness are governed by the Reynolds equation coupled with elastic deformation of the contacting surfaces. The pressure field $p(x,y)$and film thickness $h(x,y)$are obtained by solving the Reynolds equation under steady-state conditions, as commonly reported in tribological studies of rolling/sliding contacts.

The lubricant is assumed to behave as a Newtonian fluid, and isothermal conditions are considered for simplicity. The combined effects of geometry, entraining velocity, viscosity, and applied load are considered in the formulation of film thickness. To ensure consistency with earlier verified methodologies, these formulations are derived from well-known EHL models documented in the literature [relevant refs]. The main input for the ensuing stress analysis is the pressure distribution that results.

3.2. Numerical Modelling: Finite Element Analysis of Contact Stress

Subsurface stress fields and fatigue initiation tendencies in AISI 52100 bearing steel are assessed using finite element analysis using the pressure distributions derived from the EHL framework as input boundary conditions. The material is assumed to be linearly elastic and isotropic in a three-dimensional contact model, which is suitable for hardened bearing steels under mild deformation circumstances. Von Mises stress and maximum shear stress, two crucial markers for fracture initiation and propagation under rolling/sliding contact, are calculated by the FEA. Deviations from typical Hertzian stress distributions are taken into consideration because pressure anomalies (such as asymmetry and isolated spikes) can significantly alter stress magnitudes and distributions. When lubrication conditions are not ideal, this technique enables the identification of locations that are susceptible to fatigue damage.

3.3. Experimental Basis and Data Integration

To validate and support the modelling framework, Included are experimental findings for AISI 52100 bearing steel that have been documented in the literature. These include wear assessments, rolling contact fatigue test findings, and surface characterisation methods like profilometry and Scanning Electron Microscopy (SEM).

The experimental findings demonstrate wear processes (such as abrasive wear, micropitting, and scuffing) and fatigue features (such as fracture initiation and spalling) to match the expected stress fields and lubrication regimes. This integration allows for a qualitative and semi-quantitative validation of the proposed framework by linking observed damage mechanisms with suitable pressure distribution characteristics and lubrication conditions. Reputable tribological investigations on AISI 52100 bearing steel, which often used Rolling Contact Fatigue (RCF), ball-on-disc, or four-ball test setups, provided the experimental data used in this work. These studies usually report wear characteristics, friction coefficients, and fatigue life metrics (e.g., L_{10} life) based on numerous test repetitions to ensure consistency. Without conducting any new experiments, the current work synthesizes and interprets these verified datasets to show mechanical relationships between lubricating behavior and pressure distribution.

3.4. Assumptions and Boundary Conditions

To guarantee a consistent and physically significant study, the following presumptions and boundary conditions are used:

- Contact Conditions: Ball-race interaction, or concentrated contact typical of bearing elements, is considered.
- Lubrication Regime: Based on film thickness behavior and operating conditions, transitions between elastohydrodynamic, mixed, and boundary lubrication regimes are inferred.
- Sliding Condition: It is believed that pure sliding isolates the impact of anomalies in lubricant film pressure on wear and fatigue processes.
- Material Behaviour: AISI 52100 bearing steel is modelled as a linear elastic, isotropic material, which is valid under high-cycle fatigue conditions with small strains.
- Lubricant Properties: The lubricant is assumed to obey Newtonian law and incompressible, with constant viscosity under isothermal conditions.
- Boundary Conditions (EHL):
  - Inlet pressure is used as ambient pressure.
  - Cavitation is taken to account at the outlet boundary.
  - No-slip condition at the solid-fluid interface.
  - Applied normal load and entraining velocity are specified based on typical bearing operating conditions.
- Surface Effects: Although surface roughness effects are not explicitly modelled, they are taken into consideration when discussing pressure anomalies and mixed lubrication. These assumptions are consistent with recognized tribological modeling approaches and allow the identification of significant elements influencing pressure distribution and fatigue behavior.

3.5. Coupling between Theory, Simulation, and Experiment

The framework establishes a direct link between lubrication modelling, stress analysis, and experimental observations. To estimate the stress fields within the material, finite element simulations employ the pressure distributions and film characteristics provided by the EHL model as inputs. These expected stress responses are then correlated with wear and fatigue characteristics that have been discovered

experimentally and reported in the literature. This relationship enables a comprehensive knowledge of how aberrant pressure distributions impact subsurface fatigue and surface degradation processes. By integrating theoretical, numerical, and experimental perspectives, the paradigm provides a coherent basis for examining bearing failure processes under real-world operating conditions. Variations in reported wear and fatigue data are caused by differences in test settings, material preparation, and lubrication regimes, which are considered when interpreting trends.

Table 1 [Appendix] compiles the experimental configurations, material characteristics, lubrication settings, and data gathering techniques for AISI 52100 bearing steel that have been reported in the literature. The investigations frequently employ standard tribological test configurations such Rolling Contact Fatigue (RCF), four-ball, and ball-on-disc setups. Repeated trials and statistical analysis (such as L_{10} life and Weibull distributions) are used to ensure the dependability of the results. Examples of measurable parameters that are frequently acquired utilizing techniques like profilometry, interferometry, and Scanning Electron Microscopy (SEM) include wear characteristics, friction behavior, film thickness, and fatigue indicators. This systematic synthesis not only facilitates the integration of experimental evidence with theoretical and numerical modeling, but it also improves the traceability and reproducibility of the data employed in the current study.

3.5.1. Scope of the Review

This critical study integrates published experimental results on lubrication behaviour, pressure distribution, wear, and rolling contact fatigue in AISI 52100 bearing steel with theoretical developments and numerical modelling tools. No additional testing was conducted. The experimental observations discussed throughout the book are culled from peer-reviewed publications to identify common trends, knowledge gaps, and future research objectives.

3.5.2. Limitations and Uncertainty

This work inherits uncertainties related to variations in experimental conditions stated in numerous sources since it employs an integrated modeling and literature-synthesis technique. Measured metrics including wear rate, friction coefficient, and fatigue life may become scattered due to variations in material preparation, surface roughness, lubricant composition, and test configurations (e.g., ball-on-disc and rolling contact fatigue setups).

Moreover, heat effects, non-Newtonian lubrication, and plastic deformation under high loads may not be sufficiently considered by the modeling framework's straightforward assumptions. These presumptions include linear elastic material response, Newtonian lubricant behavior, and isothermal conditions. Despite these limitations, the consistency of observed trends across multiple independent trials supports the mechanical relationships between pressure distribution anomalies, lubrication regime alterations, and fatigue-wear behavior.

4. Advanced Bearing Materials and Surface Engineering for Friction, Wear, and Corrosion Control

Reducing friction and wear of rotating components are key to the efficiency, reliability and lifespan of industrial machinery, especially aerospace and high speed, machinery. Rolling-element bearings are central to this respect through the decreased contact resistance, accurate motion, and high radial and axial loads [42, 52, 53]. Nevertheless, bearing performance heavily depends on material choice which directly affects the life of bearing in terms of rolling contact fatigue, corrosion resistance, thermal stability as well as extreme operating performance [42, 54-56].

Historically, stainless steels with a martensitic composition, e.g. 440C and BG42, have been common in aerospace bearing systems, e.g. aero-engines, satellite mechanisms, and spacecraft actuators [57-64]. These steels offer a sensible compromise of hardness, strength as well as corrosion resistance. However, research has demonstrated that their intrinsic microstructure properties, including retained austenite, carbide morphology and susceptibility to localized corrosion, may be a constraint to the potential service life in adverse conditions [65-67]. In the long-term operation, they encourage surface degradation mechanisms such as pitting, stress corrosion cracking, and spalling, and eventually, impairs bearing reliability [68-70].

Studies have continued to move toward greater levels of materials and surface-engineering techniques to overcome these constraints. Because of their low density, high hardness, low thermal expansion, and superior corrosion resistance, hybrid bearings with steel raceways and Silicon Nitride (Si3N4) ceramic rolling elements have been demonstrated to function better [71-74]. Additionally, ceramic rolling elements improve fatigue life, increase lubricant life, and decrease adhesive wear and frictional heat production-all of which are especially helpful in high-speed and aircraft operations [56, 75, 76]. Additionally, surface modification techniques improve bearing durability. Physical Vapour Deposition (PVD) layers including TiN, CrN and Diamond-Like Carbon (DLC) give hard and low-friction surfaces which reduce wear and corrosion-based failures [77, 78].

These finishes enhance the behavior against rolling contact fatigue and tribochemically based degradation on the surface (particularly in the behaviour of boundaries or mixed-lubrication) [80, 81]. Meanwhile, some new bearing materials, such as high-nitrogen stainless steels, cobalt-based alloys, and High-Entropy Alloys (HEAs) are under investigation as the next generation. These materials provide high resistance to

corrosion, thermal and fatigue damage with increased resistance by alloying and microstructural stability, eliminating the long-standing weaknesses of traditional bearing steels.

The basic understanding of the mechanism of corrosion resistance underlies such developments. It was also shown by Nishimura [82] that the additions of silicon and aluminium in low-alloy steels influence the development of nanoscale complex iron oxides in the underlying rust layer and greatly enhance the rust resistance of the low-alloy steels, as well as inhibit the further development of the corrosion process. Electrochemical impedance spectroscopy showed that there were significantly higher resistances to rust and corrosion-reaction regarding the traditional low-alloy steels.

Equally, the study by Elsener et al. [83] demonstrated that nickel-free stainless steel passive films that are enriched with chromium and molybdate exhibit greater resistance to localized corrosion and that passive-film ageing results in greater resistance to pitting initiation. All these findings together represent a picture in which the control of bearing durability is not only controlled by bulk mechanical properties, but surface chemistry, passive-film stability, and control of the microstructure. Although conventional aerospace bearing steels, including 440C and BG42 have provided decades-old dependable performance, the characteristics of this category of materials also require a shift to modern-day materials and surface-engineering solutions. Longer service life, improved corrosion resistance, and dependability under more demanding operating circumstances are all made possible by these advances.

4.1. Fatigue-Driven Wear and Rolling Contact Fatigue in Bearing Steels

Rolling Contact Fatigue (RCF) is the most common cause of rolling bearing degradation throughout the course of its lifetime. Bearing steels are designed to offer optimal resistance to recurring contact stresses that develop at the raceway surface and below. According to Arakere [84], improvements in fatigue behavior, dimensional stability, inclusiveness purity, and microstructural homogeneity have been greatly enhanced by developments in steelmaking, especially high purity smelting techniques like Vacuum Arc Remelting (VAR) and Vacuum Induction Melting (VIM).The most popular bearing steel on the market is AISI 52100 (100Cr6) because of its good hardness, low cost, and resistance to rolling contact fatigue. After hardening and low-temperature tempering (Approx. 150-200°C), a typical 52100 alloy with roughly 1.0 weight percent C and 1.45 weight percent Cr generates a fine martensitic microstructure with distributed carbides.

Any remaining austenite is frequently converted using cryogenic or sub-zero (typically below -80°C) methods, which improve fatigue life and dimension stability. However, its sustained working temperature falls below 200°C due to microstructural softening and a loss of fatigue resistance [85-87]. Case-hardened steels, such as M50 NiL, can offer advantages in situations where increased toughness and thermal potential are required.

Carburizing creates a graded hardness profile with a robust, low-carbon core and high surface hardness with compressive residual stresses. Hardness values close to 750 kg/mm^2 with maintained hardness (550 kg/mm^2) at depths greater than 1.5 mm significantly improve fatigue resistance to subsurface fracture propagation and surface-initiated fatigue [85-87].

As demonstrated by Cronidur 30, nitrogen alloying has further improved fatigue and corrosion performance. These martensitic steels have low carbide volume fractions, excellent hardness, and improved corrosion resistance due to a mix of carbon and nitrogen levels between 0.6 and 0.8% wt.

High-performance applications including wind turbines, high-speed rail, and aviation engines are increasingly using these steels. Although their relatively coarse eutectic carbides may act as fatigue crack initiation, limiting rolling contact fatigue capability, traditional martensitic stainless steels, such as AISI 440C, are still used when corrosion resistance is required.

However, nitrogen-enriched martensitic stainless steels with about 13 weight percent Cr show better corrosion behavior and prevent dangerous carbide formation. Despite their higher material and production costs, high-speed steels like AISI M2 are utilized for elevated-temperature duty (>200 °C) due to their superior hot toughness. The intricate interactions between alloy chemistry, cleanliness, heat treatment, and residual stress state control fatigue-driven wear in bearings.

To prevent crack initiation and postpone fatigue propagation, modern bearing steels increasingly rely on controlled microstructures, nitrogen alloying, and graded hardness profiles. This reflects the increased significance of material design in extending bearing service life under harsh operating circumstances [85-87].

Local pressure amplification interacts strongly with non-metallic inclusions and microstructural heterogeneities in AISI 52100, promoting subsurface stress localization and accelerating crack nucleation under rolling-sliding conditions as consistent with prior studies [85-87].

At Figure 4 After dry sliding at 1 MPa and 0.2 m/s on steel 52,100, the morphology of wear products (a) and worn track (b) is studied in the case of Al7072 alloy. The tribolayer is more dispersed in some places (see arrow 2) and incredibly dense and compact in others (see arrow 1) [85-87].

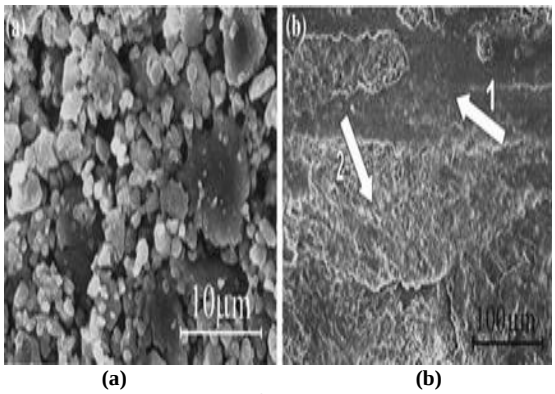

(a) (b)

Fig. 4 (a-b) Morphology of AISI 52100 steel wear [85-87]

In real-world tribological systems, wear is rarely caused by a single mechanism; rather, several wear modes frequently function simultaneously, with their relative contributions changing over the component's service life. The major wear mechanisms may alter in response to changes in operating conditions, including load, speed, lubrication regime, and surface condition.

A dynamic balance between material removal, wear particle formation, and particle removal from the interface is reflected in the resulting wear rate. Accurate wear rate prediction is intrinsically difficult because wear particle formation is affected by several interrelated factors, including as contact geometry, surface roughness, fill factor, vibration characteristics, and operating environment.

In critical applications such as bearings, gears, and precise frictional contacts, even small increases in abrasive or fatigue-related wear can have disproportionate effects on performance and reliability [85-87].

Although it may not always be the primary design driver in all mechanical systems, tribological behavior is nonetheless a significant limiting issue in many high-performance applications. The growing use of polymers, ceramics, and composite materials in addition to conventional metals in contemporary mechanical engineering, which is driven by considerations like cost, performance, and manufacturing efficiency, further broadens the scope of tribological issues. The mechanical response of contacting surfaces is governed by contact mechanics, which describes the stress and deformation fields that develop in the vicinity of loaded interfaces [88].

Classical contact configurations include concentrated and distributed normal and tangential forces, point and line contacts, and Hertzian pressure distributions under elastic loading. Studies of sliding fatigue provide important insight into related phenomena such as fretting fatigue, while analyses of plastic deformation in sliding contacts form a basis for understanding the initiation of surface damage.

Although the nominal contact area between two solids may be large, the true contact area is limited to discrete asperity junctions and increases only gradually with applied load. The formation and rupture of these asperity junctions under relative motion is commonly described by stick-slip behaviour and plays a central role in friction and wear [85-89].

A wide range of wear mechanisms has been identified, including oxidative wear, adhesive seizure, plasticity-dominated wear, and thermally induced melting. Experimental evaluation of wear behaviour is frequently conducted using simplified laboratory configurations such as the pin-on-disk test, which enables controlled comparison of materials and lubricants under defined conditions. Wang et al. [89] showed that lubricant chemistry has a significant impact on fatigue life in AISI 52100 bearing steel when it comes to rolling contact fatigue. Because of its comparatively high pressure-viscosity coefficient, synthetic polybutene (HYVIS-07) generated the longest rolling contact fatigue life among the mineral and synthetic oils examined. In general, the study demonstrated that lubricant family has a greater influence on rolling fatigue performance than viscosity differences within a particular oil type. Based on their ability to extend rolling fatigue life, the lubricants were ranked as follows: mineral oil < synthetic polybutene < synthetic polyol ester < synthetic polyalkyl glycol. Additionally, the addition of Extreme Pressure (EP) antiwear chemicals significantly increased the rolling contact fatigue life of synthetic lubricants when compared to formulations without additives. These findings show that tribological performance, particularly fatigue resistance, is controlled by the combined impacts of contact mechanics, lubrication chemistry, and surface contacts rather than merely bulk material qualities [85-89]. Table 2 [Appendix] presents various steel grades and their applications.

4.2. Deviations from Hertzian Contact and Resulting

4.2.1. Pressure Anomalies

Divergent lubricant films in elastohydrodynamic contacts are a resultant effect of an assortment of operating cooperating mechanical, thermal and chemical factors that distort ideal EHL theory classical distributions of pressure and films [103, 104]. Some of the most prevalent ones include plastic deformation, surface roughness, entrainment of debris, the formation of tribochemical films, thermal instability, lubricant starvation, and contact misalignment [105]. All these processes will cause discontinuity of the smooth, centrally peaked Hertzian-profile of pressures and the consequent wedge-shaped lubricant film and will produce local concentrations of stress and accelerated surface damage. Among the most significant reasons of abnormal film behaviour is that of lubricant starvation that takes place in instances where the supply of lubricant to the inlet part of the contact is inadequate. Starvation results in the collapse of the inlet meniscus thereby decreasing the lubricant entrained into the conjunction. This causes the central thickness of the film

to decrease and the pressure distribution to move to the film contact margins and can frequently result in dimpled or irregular shaped film shapes. Starvation is often increased by thermal effects: frictional heating of fast sliding speeds reduces lubricant viscosity, reduces the strength of the hydrodynamic wedge and further destabilises the film. Those viscosity gradients, which are caused by heat, can work to form asymmetric pressure distributions and local pressure peaks, which usually lead to scuffing or seizure [103-105].

The roughness of the surfaces creates an extra complexity of micro-Elastohydrodynamic Lubrication (micro-EHL) effects. Locally Asperities on the contacting surfaces trap lubricant and create micro-hydrodynamic films which results in high non-uniform pressure distributions with numerous local maxima. Roughness with high amplitude and short wavelength is the most undesirable type since it greatly increases the minimum film thickness and the probability of an asperity interaction. The effects encourage the spontaneous shift of full film to mixed or boundary lubrication.

Lubricant films are also distorted by third-body effects that occur due to wear debris or external contaminants [106]. The rolling or sliding of trapped particles in the contact creates localized regions of high pressure, grooves or indentations in the film shape that interferes with the nominal shape. These regions of confined pressures are stress raisers, which hasten the subsurface damage and crack initiation.

Tribochemical film formation and breakdown also add to the abnormal distributions of pressures. The surface chemistry and the local geometry of contact are altered by oxide layers or reaction films based on lubricant additives including ZDDP or MoDTC. The inhomogeneous film deposition or the inhomogeneous removal of the film re-distributes stresses in an uneven manner on the contact, creating local pressure hot spots that are not predicted by classical EHL [107]. Contact geometry may also permanently or temporarily vary, which also affects pressure distribution. High subsurface stresses lead to plastic deformation of asperities or elastic bulging that changes the conformance of the contact loads by moving load support off-centre to contact shoulders and creating bimodal or asymmetric pressure profiles.

Likewise, edge effects and misalignment, caused by surface waviness, angular misalignment, assembly, tolerances of assembly, cause edge loading, where the pressure is concentrated on only one side of the contact, resulting in very asymmetric films and high local stresses [88, 107]. The combination of these processes shows that abnormal lubricant film behaviour does not occur due to one perturbation, but due to the cooperating effects of mechanical, thermal, chemical, and geometric actions. These non-ideal behaviour of EHL have been critically linked and related to the pressure and accelerated wear and early fatigue of rolling contacts, and it is vital to comprehend and manage pressure and film irregularities in high-performance bearing application.

4.2.2. Rolling Contact Fatigue Modes and their Dependence on Lubrication and Pressure Distribution

Sadeghi et al. [108] provided a detailed overview of Rolling Contact Fatigue (RCF) mechanisms and identified two different modes of fatigue surface and subsurface initiated respectively, and a map of the operating regime and pressure that favour either. They also pointed out that rolling-element bearings represent one of the most used machine elements, and that subsurface-initiated spalling, which develops due to cyclic Hertzian stresses, is one of the most common forms of failure when operating well-lubricated. Their review pointed to decades of studies which are directed at understanding the RCF mechanisms and formulating fatigue-life prediction models, along with finding the weaknesses of classical approaches as well as the necessity of better mechanistic models.

Expanding on this difference, Santus et al. [109] investigated the factors which drive the transition between subsurface and surface damage modes between subsurface-initiating spalling and surface-initiating pitting and micropitting. They observed that unequivocally, in situations of scuffing and gross lubrication failure inhibited, RCF is the damage mechanism of last resort in Hertzian contacts, such as cams, gears, and rolling bearings. In contrast to traditional fatigue, RCF is initiated under compressive, multi-axial, non-proportional, and very non-uniform stress state, unlike when tensile loading is involved. Santus et al. also differentiates between fatigue response of softer steels in which cyclic ratcheting and plastic shakedown are predominant, and high strength bearing steels, including AISI 52100, in which elastic shakedown prevails with damage building up through microstructural evolution. Cyclic shear stress indices were used to classify and link both surface- and subsurface-initiated RCF mechanisms to characteristic depths, which allowed better correlation of laboratory results and component-scale behaviour. Abdullah and Khan [110] further underlined the susceptibility of rolling bearing components to microstructural development under the influence of RCF with the argument that it is difficult to model fatigue damage on a multiscale basis. The composition of steels, non-metallic inclusions, the development of residual stress, and the competing influences of strain hardening and softening are some of the factors making it difficult to predict fatigue-life. Although significant focus has been placed on the process of modelling subsurface-initiated fatigue, there has been comparatively little consideration with regards to the dynamic development of near-surface microstructures during situations that do not follow ideal lubrication and pressure field distributions in EHL behaviour. The instability of lubrication contributes to the promotion of surface-initiated RCF. By showing that lubricant starvation is a major risk factor in causing surface distress and micropitting, the study by Poll et

al. [111] showed that the thickness of the film and pressure generation in the contact was reduced. They observed rolling-element bearings often tend to run with starved conditions resulting in inadequate pressure accumulation and reduced film protection. In line with this, Meng et al. [112] detected the effects of thermal EHL, starving EHL and surface roughness as major causes of wear transitions in lubricated contacts. Several reviews have also provided a further clarification of the process by which abnormal pressure distributions relate to surface degradation. Wang et al. [89] demonstrated that sliding and mixed lubrication conditions facilitates the change of micropitting to macropitting of steel gears with the aid of asperity-scale-stress amplification and crack formation. The authors Patel et al. [114] linked surface-initiated cracking, micropitting, and wear transitions, such as scuffing, to collapse of lubricant films and the following spikes of pressure at the asperity contacts. Lugt [115] presented a comprehensive study on how the film forming at the inlet side was studied with attention being given to the way starvation of the inlet and thermal effect altered the pressure and traction distribution and made bearings and gears more prone to surface damage. Cheng [116] described classical transitions between EHL and mixed and boundary lubrication, showing that the sudden change in temperature or pressure can cause the transition between mild wear and severe scuffing.

The amplified local pressure due to roughness behavior under both rolling-sliding conditions was further stressed by Morales-Espejel [117] who attributed these effects to the actual nucleation of surface cracks, micropitting, and scuffing. A definitive treatment of surface initiated RCF was achieved by Olver [118], who described how cyclic stresses near the surface, which is enhanced by friction, roughness, and sliding, leads to the development of microcracks and pits or spalls. Snidle et al. [119] established that systems can change to scuffing in the event of localized pressure and flash temperature spikes due to changes in loads, poor film formation, or large slide to roll ratios. Most recently, Wainwright and Kadiric [120] applied operating-condition maps to compare the relationship between contact pressure and sliding severity with the initiation of microcracks and the advancing pitting and micropitting damage.

Taken together, these investigations indicate that material properties and Hertzian stress fields are only controlling factors of RCF behaviour, but the stability of lubricant films and the consequent pressure distributions. Differences between classical EHL, such as due to starvation, thermal effects, roughness or sliding, cause fatigue damage to lie not in subsurface-initiated spalling but in surface-initiated cracking and micropitting. This change applies especially to high strength bearing steels like AISI 52100 where an abnormal distribution of pressure increases the rate of near-surface fatigue and shortens bearing life by a considerable margin.

4.2.3. Lubrication Regimes, Sliding Severity, and Wear-Fatigue Transitions in AISI 52100 Bearings

The lubrication regime in rolling and sliding contacts is usually identified by the film parameter

$$\lambda = \frac{h_{\min}}{\sigma} \tag{3}$$

Where $h_{\min}$ is the minimum lubricant film thickness and $\sigma$is the composite surface roughness [121]. When $\lambda > 3$, full Elastohydrodynamic Lubrication (EHL) is confirmed, asperity interactions are insignificant, and the risk of micropitting is negligible. In the mixed lubrication regime ($1 < \lambda < 3$), intermittent asperity contact occurs, significantly increasing predisposition to micropitting. When $\lambda < 1$, boundary lubrication prevails, and adhesive wear, abrasive wear, and scuffing become the dominant damage modes. Besides the thickness of the film, the Slide to Roll Ratio (SRR) has a deforming effect on the wear and fatigue transitions.

Micropitting initiation is mainly dominated by surface roughness and cyclic stress fields beneath the surface under rolling dominated conditions (SRR 0-5%). Increased frictional shear at intermediate levels of SRR (10-30%) will facilitate surface induced fatigue cracks and rapid progression of mild wear into severe damage.

When the sliding ratio is very high (SRR > 50%), the starvation and thermal wedge effects prevail, and can often cause scuffing or scoring. The nominal Hertzian contact pressures in rolling bearings are usually in the range of 0.8-1.5 GPa. Nevertheless, it is possible to have local asperity contact, loading at the edges, or retention of debris, which results in pressure spiking more than twice the nominal Hertzian pressure, and provides favourable crack initiation conditions in AISI 52100.

The misalignment or waviness of pressure fields also increases the occurrence of cluster of microcracks especially at the surface. The supply of lubricants is critical in ensuring that the film is stable or collapses. The inlet meniscus collapse, central film thinning and speeding up of the micropitting is seen in partial starvation and central film being uniform in pressure with more stable central films in the case of fully flooded conditions. In extreme starvation with excessive sliding, wear changes to scuffing are usually apparent.

Those effects are highly enhanced due to thermal effects: local flash temperatures of 50-70°C at the bulk oil temperature can have a severe impact on the viscosity of lubricants, distort pressures distributions, and the weakening of the hydrodynamic wedge. The ongoing shear heating can also promote the thermal wedge effects and increase the initiation and propagation of the cracks. The modulations of these processes are critically dependent on surface roughness

characteristics. Roughness of large amplitude in short wavelength (e.g. R_a > 0.2 μm) forms sharp local pressure peaks, and decreases minimum film thickness, which encourages micropitting. Conversely, waviness of longer wavelengths is likely to cause edge loading and surface-initiated fatigue. In line with the micro-EHL research, there is an insignificant effect of roughness phase angle on minimum film thickness [48]. The debris and third-body particles further enhance the damage by creating transient and localized high-pressure events promoting micropitting and changing the wear to abrasive regimes.

As a result, the methods of rubbish monitoring, like ferrography, can be useful in the detection of atypical wear transitions at the initial stages. These interdependent effects may be summarized by a wear-fatigue mode map, where the lubrication regime, SRR, pressure distribution, and thermal effects are combined to define the development of damages. Extreme starvation coupled with high sliding conditions are conducive to scuffing and other transition to adhesive and abrasive wear, abnormal local pressure distributions are conducive to asperity fatigue and micropitting, and extreme high shear at intermediate levels of SRR are favourable to surface-initiated cracks which may subsequently develop to macropitting.

For AISI 52100 bearing steel, these insights highlight the importance of maintaining stable lubricant films and controlled sliding conditions to delay fatigue initiation. Common practices reported to mitigate damage include limiting SRR below approximately 10% in critical bearings, ensuring adequate lubricant replenishment to prevent inlet starvation, and maintaining $\lambda \gtrsim 2$ through appropriate lubricant viscosity selection and surface superfinishing (e.g., Ra<0.05 μm). By monitoring friction and temperature transients, additional early warning of anomalous film behavior and impending wear or fatigue transitions can be acquired.

The dynamic coupling between the behavior of the lubricant film and the distribution of the contact pressure is a dynamically coupled system that controls the transition between lubrication regimes and failure modes, and not just a passive tribological response. Under conditions of ideal Elastohydrodynamic Lubrication (EHL), a stable lubricant coating maintains sufficiently good separation between asperities; but on introduction of anomalies in pressure, such as localized spikes, skewed distributions, and transitory collapse regions fundamentally change this equilibrium.

These anomalies cause a locally thinning of the lubricant film, which reduces the film parameter (ratio of λ) and promotes the shift between full-film EHL and mixed or boundary lubrication regimes. This transition is critical because the onset of direct interaction of the *asperities*, leading to the rise of frictional heating, surface distress and rates of materials loss by a significant margin. Subsequently, pressure irregularities work as precursors and accelerate wear processes and initiate microstructural damage in the bearing material as opposed to acting in isolation.

4.3. Analysis and Discussion

4.3.1. Wear and Fatigue Behaviour under Pressure Anomalies

A key method employed by researchers to establish a relationship between the development of wear transitions, surface-initiated cracks, and micropitting to aberrant pressure distributions (local peaks, starvation, edge-loading, and asperity contacts) is fatigue-life mapping [121, 122]. Weibull probability charts are often used to represent the scatter in Rolling Contact Fatigue (RCF) life in bearing fatigue research. The parameter of the scale (η) represents the mean life, and the slope (β) represents the variability.

Performance of greased or rolling contact fatigue has been correlated with anomalous pressure distributions (caused, e.g., by asperity stress, hunger, thermal effects, or gradient material structures) in a variety of notable studies through fatigue-life mapping [123-126]. Typically, this is done using Weibull plots or PVt (Pressure × Velocity × time) metrics. Researchers found a distinct fatigue limit at about 3 GPa in a study on rolling contact fatigue in 32CrMoV13 nitrided steel: contacts under that Hertzian pressure had a long life (> 10^6 cycles).

Additionally, a lower fatigue life (less than 10^5 cycles) was the outcome of higher pressures [127]. Weibull parameters were used to quantify fatigue performance in a similar work on grain refinement. The scale parameter η (characteristic life) showed a power-law dependency on contact pressure and grain diameter, whereas the shape parameter β (scatter behavior) increased as grain size dropped. This led to the development of a predicted two-parameter Weibull fatigue life equation that established a direct relationship between life expectancy and pressure and material microstructure. Zhao et al. [128] developed a subsurface fatigue model that included cyclic hardening gradients in bearing steel.

The model successfully predicted RCF life using Weibull statistics to characterize the survival probability of microstructural volume elements under different stress cycles by combining stress-state calculations with subsurface performance disparity. Researchers looked at the Weibull slope (β) in addition to the standard bearing life parameter, L_{10}, in bearings with altered residual stress states. Significantly longer lifetimes (from 274-1924 hours) were demonstrated by hard-turned and deep-rolled bearings, which were associated with more advantageous pressure distributions and subsurface stress profiles brought about by finishing procedures [127, 128]. Researchers created tribo-fatigue damage maps by testing under various tangential (sliding) forces and contact pressures, even though bearing-specific PVt-to-life correlations are less frequently explored.

They used wear rate and crack length vs stress history to categorize damage into "slight," "fatigue," and "severe fatigue" regimes-basically, a PVt-type mapping technique. The sensitivity of AISI 52100 to contact circumstances and lubricant chemistry has been measured using life statistics (L_{10}/Weibull) in several multi-ball/extended RCF experiments.

To demonstrate that scale/shape parameters change systematically with contact stress and processing (heat treatment, residual stress), researchers fitted 2- or 3-parameter Weibull distributions to RCF S-N data. PVt maps are used to correlate operational regime to observed damage mode. Reviews and experimental publications map damage severity vs. contact pressure and sliding to indicate regime borders. Micropitting reviews and experiments on AISI 52100 demonstrate that surface cracks and life reduction are driven by local pressure amplification and film collapse. A useful method of measuring how "abnormality" reduces life is to combine Weibull statistics with mechanistic measurements (local peak pressure ratio, kurtosis of reconstructed p (x, y), or PVt bins).

Researchers typically combine the following elements such as controlled RCF testing (AISI 52100 test balls, rings, and races) in a matrix of temperature, surface finish, lubrication condition (flooded vs. starved), sliding (SRR or sliding speed, U_s), and nominal Hertzian pressure (P_o). Cycles to initiation, also known as L_{10} or spall events, are used to document life. Each test's damage is categorized as either micropitting, pitting, scuffing, spalling, or no damage. The mechanism is confirmed by 3D profilometry and microscopy. Fit two- or three-parameter Weibull distributions to the cycles-to-failure data for every condition or bin to perform statistical life analysis. Extract the shape β (scatter), the scale parameter η (characteristic life), and occasionally the location γ. Compare conditions and plot survival functions.

Oxidative Glaze Layers: Thin tribo-oxidative coatings made typically of Fe-oxides (FeO_3, FeO_4) are formed by AISI 52100 at moderate sliding and continual contact temperatures (Approx. 100-200°C). These develop because of oxygen intrusion from lubricant degradation and localized flash heating. Smooth, glazed surface with a blueish or brownish colour for the morphology. Finely compacted oxide particles and oxygen enrichment are frequently seen using SEM/EDS. The steel matrix is linked to a thick, protective oxide scale in cross-sections.

Impact on performance can reduce direct asperity-asperity contact by serving as a protective, sacrificial layer. But after breaking, brittle oxides can function as third-body abrasives and contribute to plough wear. Oxidative glazing frequently works as a self-limiting agent by stabilizing at constant, moderate pressure and temperature [129]. Abrasive Ploughing: occurs when the interplay between asperity and asperity (low λ, mixed/boundary lubrication) is dominant. Three-body abrasion results from the entrainment of hard debris particles (broken oxides, inclusions, and counterface transfer). Parallel grooves or furrows that were in line with the direction of sliding were seen in the SEM for the morphology. Grain elongation and a plastically distorted subsurface are visible in cross-sections close to grooves. Secondary micro-cutting is frequently caused by debris fragments re-embedding.

The impact on output increases surface roughness and, through the concentration of stress, speeds up the beginning of micropitting. causes particles to clog the contact inlet, which leads to lubrication hunger. Localized pressure spikes (asperity contacts > 2× Hertz pressure) are highly associated with abrasive ploughing [130]. Scuffing (Adhesive Wear Transition): It is activated by high flash temperatures (>200 °C), film collapse ($\lambda < 1$), and a high Sliding/Rolling Ratio (SRR > 30-50%). When lubricant coating degrades, metal-to-metal connections occur. Catastrophic damage results from the welding and tearing of adhesive connections during sliding. Large areas of smeared, plastically flowing material with tearing evidence are indicative of the morphology. SEM shows surface smearing or features that have melted or resolidified.

From welded joints, microcracks spread outward and frequently combine to form macro-spalls. The impact on output represents a significant change in wear mode: failure occurs quickly when scuffing starts. frequently accompanied by abrupt temperature spikes and aberrant traction curves. Scuffing: Immediately related to applying pressure when shear amplification occurs due to edge/misalignment, sliding concentration, or lubricant deprivation. Oxidative glazing predominates for the AISI 52100 at lower tension and sufficient oil.

Debris-induced abrasive plowing occurs when the film thins ($\lambda < 2$). When overload, famine, or sliding spikes occur, scruffing suddenly takes over, resulting in catastrophic collapse [127-132]. Figures 5-8 present the SEM-style images illustrating typical wear morphologies relevant to AISI 52100 bearing steel under rolling-sliding contact conditions. The SEM features for the oxidative glazing reveal smoother areas with a glassy, flowing texture, occasionally accompanied by delamination or tiny cracks.

EDS/TEM Perspectives: high oxygen level, which results in the formation of dense oxide layers (FeO_4/FeO_3). Under the glazing, there is usually little subsurface deformation. Figure 5 illustrates how the SEM features for the abrasive ploughing display parallel micro-grooves/furrows that are in line with the direction of sliding. Elongated grains beneath these grooves, plastic deformation on the subsurface, and a high Kernel Average Misorientation (KAM) in EBSD all point to the location of stress.

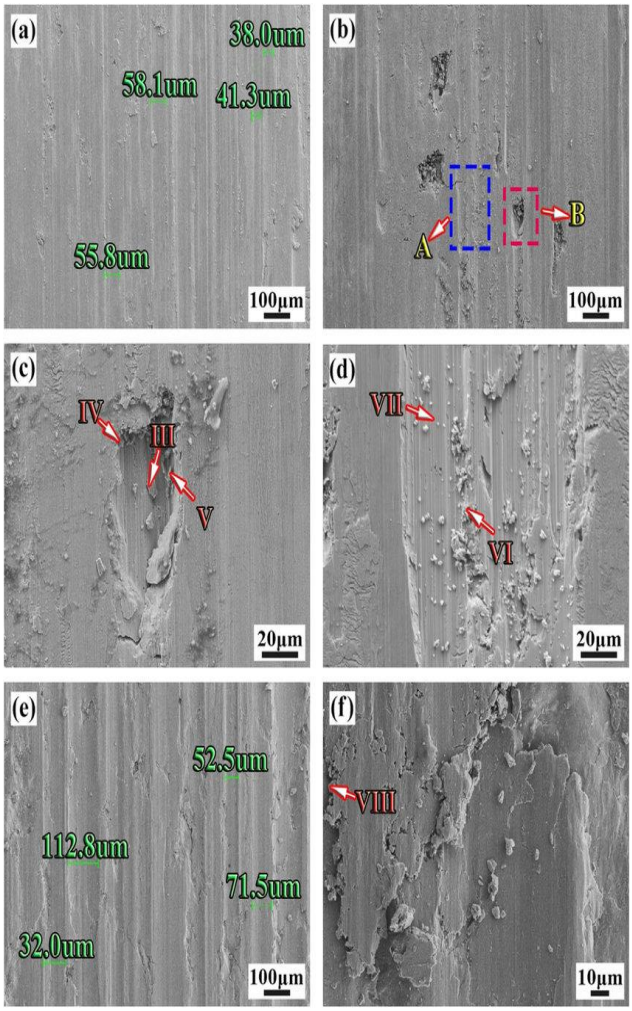

Fig. 5 Clear abrasive ploughing grooves-fine, linear scratches aligned with sliding direction [129-132].

The SEM features for the early scuffing/mixed wear reveal embedded debris together with combined ploughing and surface breakdown (e.g., manners illustrated in Figure 6). Subsurface: Possible fatigue crack sources, strain building, and the onset of microcracks. Figure 7 illustrates the SEM features for the Scuffing (Severe Adhesive Wear), which include smear-like surface flow, surface melting, or material transfer layers.

White Etching Bands (WEBs), Dark Etching Regions (DERs), residual austenite transition, and local softening brought on by flash heating are all visible beneath the surface. Table 3 [Appendix] shows the research done on AISI52100 [131-137]. Mild wear under partial film separation is indicated by the fine abrasive grooves in Figure 5 that are aligned with the sliding direction. On the other hand, Figure 6 shows surface breakdowns and wider ploughing tracks, indicating a shift toward severe mixed or boundary lubrication conditions caused by pressure-induced film collapse.

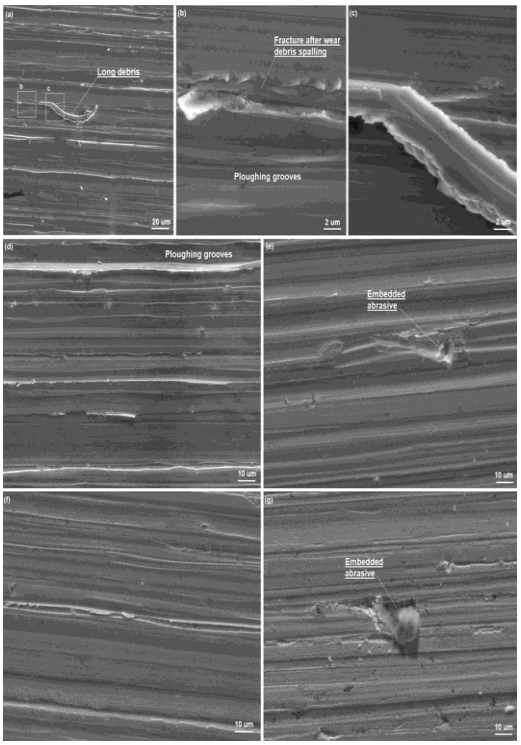

Fig. 6 Mixed abrasive wear patterns with embedded debris fragments and micro-grooves [130, 131, 133]

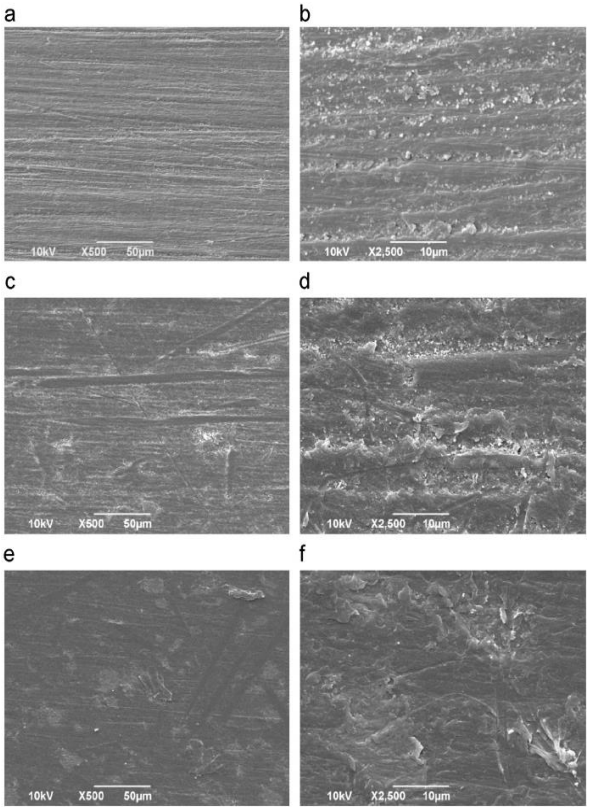

Fig. 7 Broader wear tracks showing signs of ploughing and partial surface breakdown, indicative of onset scuffing [134-137]

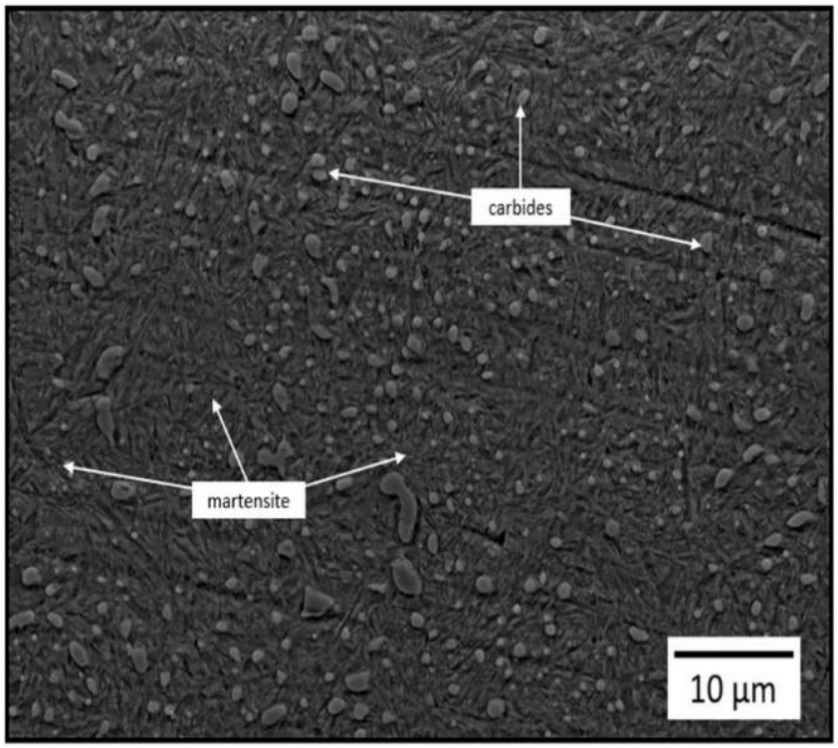

Fig. 8 Surface features resembling initial oxide formation/glaze, or smoothed wear zones [128, 137]

Table 3 [Appendix] presents a summary of the previous research and shows a consistent correlation between variation in the lubrication regimes, anomalies in pressure distribution and the fatigue-wear results of AISI 52100 bearing steel. Both experimental and modeling studies show that localized amplification of pressure and non-Hertzian distributions of stress are the result of deviations of ideal elastohydrodynamic conditions, such as thinning of the film, hunger, and surface roughness effects. These pressure anomalies are well related to the development of micropitting, surface crack formation and decreased fatigue life. Most importantly, the data indicate that, despite the potential surface engineering techniques and lubricant additives to mitigate some of these effects, they do not eliminate the underlying pressure-driven damage mechanisms, in particular, in mixed and border lubrication regimes. This synthesis, therefore, underscores the need to have combined approaches that explicitly consider pressure abnormalities in predicting wear and fatigue behavior.

The synthesized data in Table 3 [Appendix] demonstrate a continuous and mechanistically significant relationship between changes in lubrication regime, anomalous pressure distribution and fatigue-wear behavior in the AISI 52100 bearing steel. One consistent trend in the studies examined is that an amplification of localized pressure and non-Hertzian contact behavior are due to the degradesment of ideal Elastohydrodynamic Lubrication (EHL) conditions, including lubricant starvation, effects of surface roughness and additive-dependent film instability.

These pressure anomalies are most commonly manifested through film thinning and asymmetric pressure profiles, as well as localized spikes in pressure. Among the significant conclusions reached on the basis of the data is the fact that a critical temperature determining the beginning of the process of failure is the transition of full-film EHL to mixed lubrication. Fatigue damage under stable EHL conditions is mainly subsurface-driven and in agreement with classical Hertzian stress forecasts. But the dominance of asperity contact provides very localized stress concentrations that accelerate dramatically surface initiated damage mechanisms as the lubrication regime approaches mixed or boundary conditions. Based on multiple studies shown in Table 3 [Appendix], mixed lubrication is always associated with micropitting, surface cracking, and early-stage spalling. Hunger and micro-EHL effects caused by roughness contribute to the worsening of this behavior.

Also, the data indicate that with the help of a feedback mechanism, the pressure anomalies do not only cause damage but also contribute to its development. Localized wear alters the surface topography to enhance pressure concentration and promote additional film breakdown. This association between surface damage and pressure redistribution, which ultimately causes fatigue life to be shorter than predicted by considering the nominal contact stress. The effectiveness of lubricant additives such as WS_2 and MoS_2 have some efficacy in reducing friction and delaying the development of cracks, but are limited in extreme conditions when collapsing of the film

due to pressure is the main cause. The combination of the interpretation of the data demonstrates that the stability of lubricant film and the presence of the irregularities of the pressure play a significant role in determining the fatigue life in the AISI 52100 bearing steel in addition to the material characteristics and the nominal loading circumstances. The findings emphasize the importance of considering non-ideal pressure distributions and transitions between lubrication regimes in bearing performance prediction models because these factors are critical to the development and progression of wear and fatigue failure in operating under real-world operating conditions. Common aberrant signatures observed in different studies include edge/misalignment peaks, thermal-wedge-driven skewed films, roughness-driven micro-EHL pressure spikes, and inlet starvation (dimpled/collapsed inlet). Micropitting, surface cracking, or fast wear transitions are always preceded by these signs. According to AISI 52100-specific experiments [31, 89], lubricant chemical and feeding condition significantly alter life, mostly through modifications to local pressure anomalies and film thickness. The aberrant pressure measures (p_spike ratio, λ, and PVt) can be statistically connected with the risk of failure or life through the use of modeling and Weibull/PVt techniques [110, 114, 138].

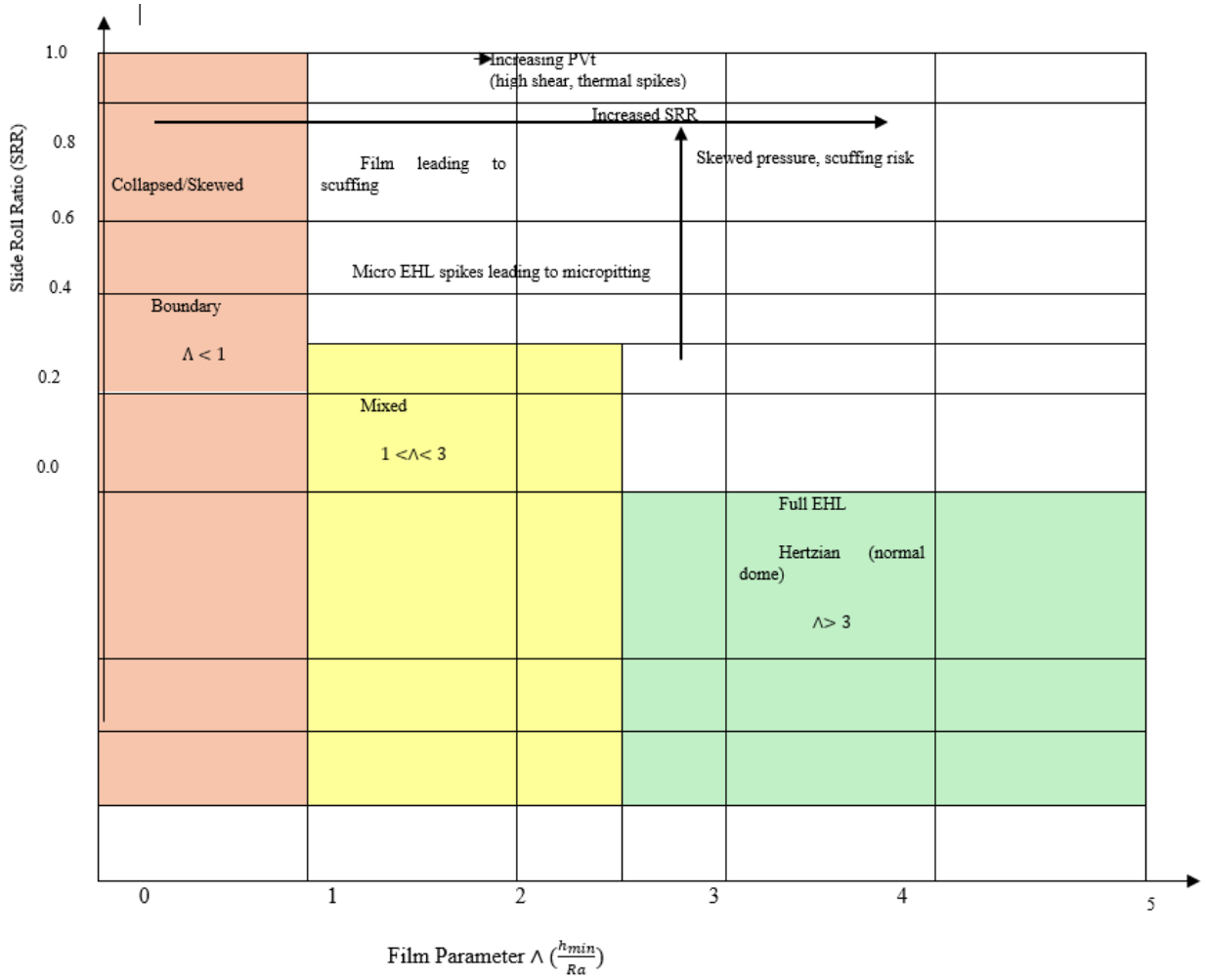

Fig. 9 Schematic "map" linking lubrication regimes to pressure distribution and failure modes for AISI 52100 [140]

The film parameter, Λ, as presented in Figure 9 determines if the EHL regime is full-film, mixed, or boundary. Scuffing concerns are increased by the pressure dome's skew caused by the Slide-Roll Ratio (SRR). Micro-EHL or scuffing transitions are caused by shear/thermal spikes driven by PVt (Pressure × Velocity × Time). Fatigue-dominated existence with a Hertzian dome is implied by full-film EHL (Λ > 3). Micro-EHL spikes and micropitting are implied by the mixed regime (1 < Λ < 3). Boundary (Λ < 1) shows twisted or collapsed Scratching films [139, 140]. The schematic mapping shown in Figure 9 offers a coherent framework that connects lubrication regimes, the characteristics of pressure distribution and the predominant mechanisms of failure in AISI 52100 bearing contacts. Instead of considering the elastohydrodynamic, mixed, and boundary lubrication regimes as discrete states, the figure depicts a continuum,

controlled by the fact that the lubricant film integrity deteriorates as pressure aberrations and sliding severity increases. The pressure distribution in the full-film EHL regime is relatively smooth and Hertzian-like, to favour subsurface-dominated fatigue with minimal surface damage. However, when localized pressure anomalies become increasingly severe, i.e. when localized spikes and asymmetric distributions begin to occur, the system transitions into mixed lubrication, where partial film breakdown starts to take place, leading to both simultaneous activation of surface wear (abrasive and adhesive) and subsurface crack initiation. In the boundary regime, intense film collapse leads to predominant asperity interaction which causes rapid surface degradation, scuffing, and enhanced crack propagation.

Notably, the map emphasizes that fatigue life does not necessarily entirely depend on transitions of lubrication regimes but is heavily influenced by the interaction between transitions of lubrication regimes and stress concentrations because of pressure. This combined representation thus gives a more realistic predictive model of bearing failure at non-ideal operating conditions.

A mechanistic view of fatigue-life degradation in abnormal pressure distributions demonstrates that there is a strong coupling between surface and subsurface failure mechanisms. High localized pressures enhance the magnitude and gradient of subsurface shear stresses and thereby accelerate crack nucleation in regions underneath the contact surface, especially in high-carbon steels such as AISI 52100. At the same time, the degradation of lubricant film integrity will increase asperity contact, leading to abrasive and adhesive wear, as shown in Figures 5-8. This twofold activity creates a feedback mechanism whereby surface damage will change contact geometry, which in turn will distort the pressure distribution and increase the stress concentrations. Consequently, the life of fatigue is not only controlled by the classical Hertzian predictions of stresses, but it is also greatly diminished by the existence of pressure-induced anomalies and transitions in lubrication regimes. The fatigue-life mapping in this study is therefore a more realistic representation of bearing performance based on integrating the characteristics of pressure distribution and the wear evolution and crack propagation behaviour thus providing a more comprehensive framework on which the predictive premature failure in the practical application can be performed.

The analysis of the synthesized evidence outlined in Table 3 [Appendix] and interpreted alongside the lubrication-fatigue framework in Figure 8 shows a consistent correlation between the transitions between the lubrication regimes, the anomalies of the pressure distribution, and the fatigue-wear behaviour in AISI 52100 bearing steel. Deviations of ideal Elastohydrodynamic Lubrication (EHL) (such as starvation, roughness effects and film breakdown) are continually related to localized pressure spikes and non-Hertzian stress fields, which serve as primary contributors to damage initiation. Bearing behaviour, as shown in Figure 9, is continuously changing between full-film EHL and mixed and boundary lubrication regimes. When pressure distributions are smooth in the EHL regime, the subsurface fatigue will have minimal surface damage. Tables 3 and 4 [Appendix] however reveals that after film instability has taken place, a mixed lubrication condition has been established and hence, asperity contact, micropitting and surface cracking have taken place. Under boundary lubrication, extreme film collapse leads to concentrated contact pressures, accelerated wear, and scuffing, and is a sign of accelerated failure. Notably, both Table 3 [Appendix] and Figure 9 emphasize the presence of a feedback mechanism, whereby initial surface damage changes contact geometry, further enhancing the degree of non-uniformity in pressure, and further accelerating the path of fatigue progression. This interaction accounts for the measured reduction in fatigue life at non-ideal lubrication conditions and that bearing failure is controlled not only by nominal stress but also by the changing pressure distributions and the instability in the lubrication regime. In the ideal conditions of elastohydrodynamic lubrication, coefficient of friction as low as +0.02 has been reported, which corresponds to a stable film separation and a minimum surface interaction. But, as can be seen in Tables 3, 4 [Appendix] and Figure 9, the shift to mixed lubrication because of pressure anomalies results in a dramatic increase in asperity contact, which is associated with the increased wear rates and the accelerated onset of fatigue. This analogy indicates the non-optimal behaviour of lubrication and points to the effect of irregularities in pressure distribution on the degradation of performance. The falling of the lubricant film thickness under starvation or roughness effects can alter the film parameter (λ) to being less than 1 (mixed lubrication) and cause a significant increase in the risk of micropitting and initiation of surface cracks. Compared to state-of-the-art approaches, which often analyze lubrication behaviour, wear evolution, or fatigue mechanisms independently, the present framework provides a coupled interpretation that captures the interaction between pressure distribution anomalies and material response. As shown in Table 3 [Appendix] and Figure 9, existing studies typically report either surface damage features or fatigue life trends without explicitly linking them to non-Hertzian pressure effects. By integrating EHL-based pressure prediction with stress analysis and experimental evidence, this study is able to explain the transition from stable lubrication to mixed and boundary regimes in terms of pressure-induced film breakdown and stress concentration. This makes it possible to anticipate failure progression more accurately, especially when it comes to identifying early-stage fracture initiation caused by localized pressure spikes-a feature that traditional models do not specifically address. Consequently, the proposed approach provides improved insight into fatigue-life degradation mechanisms under non-ideal operating conditions.

5. Corrosion Mechanisms in Bearing Steels

Corrosion represents one of the most critical degradation pathways for rolling-element bearings operating in aggressive environments such as aerospace, marine, wind-energy, and high-humidity applications [141-143]. High-carbon chromium bearing steels, most notably AISI 52100, are widely used because of their excellent hardness, wear resistance, and rolling contact fatigue strength.

Besides the thickness of the film, the Slide to Roll Ratio (SRR) has a deforming effect on the wear and fatigue transitions [144-147]. Micropitting initiation is mainly dominated by surface roughness and cyclic stress fields beneath the surface under rolling dominated conditions (SRR 0 -5 percent) [113, 148-153]. Increased frictional shear at intermediate levels of SRR (10 30%) will facilitate surface induced fatigue cracks and rapid progression of mild wear into severe damage. Starvation and thermal wedge effects prevail at extremely high sliding ratios (SRR > 50%) and often results in a scuffing/ scoring [154, 155].

The nominal Hertzian contact pressures in rolling bearings are usually in the range of 0.8-1.5 GPa [156, 157]. Nevertheless, it is possible to have local asperity contact, loading at the edges, or retention of debris, which results in pressure spiking more than twice the nominal Hertzian pressure, and provides favourable crack initiation conditions in AISI 52100 [158, 159]. The misalignment or waviness of pressure fields also increases the occurrence of cluster of microcracks especially at the surface [160]. The supply of lubricants is critical in ensuring that the film is stable or collapses. The inlet meniscus collapse, central film thinning and speeding up of the micropitting is seen in partial starvation and central film being uniform in pressure with more stable central films in the case of fully flooded conditions.

In extreme starvation with excessive sliding, wear changes to scuffing are usually apparent. Those effects are highly enhanced due to thermal effects: local flash temperatures of 50-70°C at the bulk oil temperature can have a severe impact on the viscosity of lubricants, distort pressures distributions, and the weakening of the hydrodynamic wedge. The ongoing shear heating can also promote the thermal wedge effects and increase the initiation and propagation of the cracks [161, 162]. These processes are vital processes that are modulated by surface roughness characteristics. Roughness of large amplitude in short wavelength (e.g. R a >0.2mu m) forms sharp local pressure peaks, and decreases minimum film thickness, which encourages micropitting. Conversely, waviness of longer wavelengths is likely to cause edge loading and surface-initiated fatigue. In line with the micro-EHL research, there is an insignificant effect of roughness phase angle on minimum film thickness [48]. The debris and third-body particles further enhance the damage by creating transient and localized high-pressure events promoting micropitting and changing the wear to abrasive regimes. As a result, the methods of rubbish monitoring, like ferrography, can be useful in the detection of atypical wear transitions at the initial stages. These interdependent effects may be summarized via a wear-fatigue mode map, where the lubrication regime, SRR, pressure distribution, and thermal effects are combined to define the development of damages.

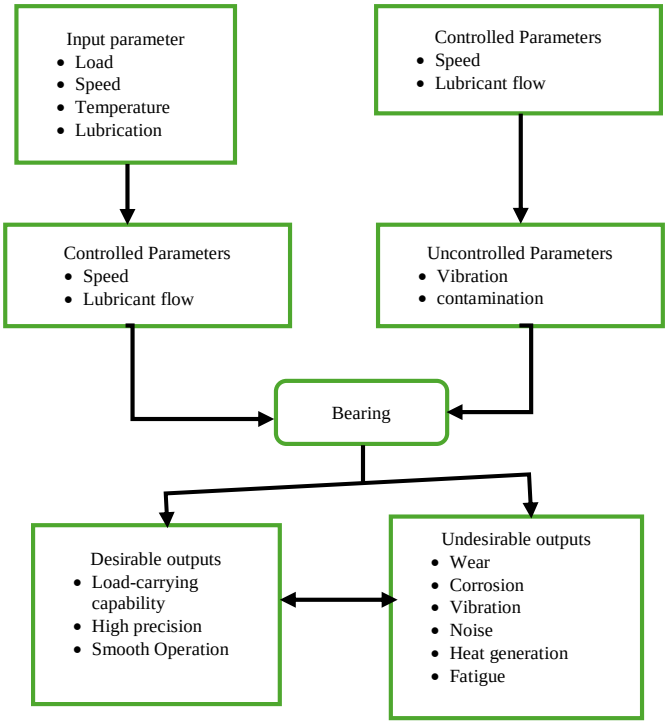

Fig. 10 Operating and response variables of bearings [163]

Extreme starvation coupled with high sliding conditions are conducive to scuffing and other transition to adhesive and abrasive wear, abnormal local pressure distributions are conducive to asperity fatigue and micropitting, and extreme high shear at intermediate levels of SRR are favourable to surface-initiated cracks which may subsequently develop to macropitting. Recent studies have given more attention to the implementation of machine learning algorithms and artificial neural networks and more advanced signal-segmentation techniques to optimize and enhance both traditional and new mechanical systems. As shown in Figure 10, the frameworks of bearing defects detection often use measured parameters of vibration, acoustic signals, operational signals, and environmental/chemical signals based on which machine learning models forecast the resultant parameters in the form of fault identification, defect severity, corrosion-related degradation, and the general bearing health state, which will be accurately diagnosed without causing further damage.

6. Heat-Treatment Studies of Selected Bearing Steels

Like the case of heat-treatment, experimental results continually reveal that the ultimate behavior of bearing steels such as hardness, Rolling Contact Fatigue (RCF) life, wear resistance, dimensional stability and corrosion or temperature resistance is not determined by alloy chemistry but the overall processing path.

According to the industrial reviews by Schaeffler [95], the critical variables are smelting and refining cleanliness, austenitizing temperature and soak time, quenching medium and severity, tempering schedule, and immediate use of special treatments, e.g., cryogenic stabilization, carburizing or nitriding and remelting processes (e.g. ESR, VAR, PESR). A combination of these parameters is vital in providing successful performance under extreme service conditions of bearing.

Throughout the literature, strategies of heat-treatment of bearing steels are aimed at achieving a number of common objectives: (i) creation of a martensitic matrix with a fine and well-dispersed carbide population to achieve the highest possible wear resistance and fatigue strength; (ii) reduction in retained austenite and chemical segregation by clean melting and controlled melting; (iii) control of core toughness and thermal stability by suitably tempering; and (iv) the use of surface or case treatments when increased wear resistance, fatigue strength, or corrosion protection is Much of the retained austenite reduction, refinement of martensitic substructures, fine carbide precipitation, and increase in dimensional stability and contact fatigue life are largely attributed to cryogenic processing and multiple tempering cycles, primarily of aerospace bearing steels of high-performance, like M50 and M50NiL [164, 165]. In typical heat-treatment paths of more traditional through-hardened bearing steels like AISI 52100 (100Cr6), austenitizing at around 820-860°C then oil quenching and the low to moderate temperature tempering is used to achieve hardness levels of between HRC 58 and HRC 64.

When well processed, this creates a martensitic microstructure whereby the carbides are well dispersed giving it superior wear resistance and RCF behavior at a modest cost. But, according to Blass et al. [166], the comparatively low level of chromium limits corrosion resistance, and the hardness stability decreases at about 120 -150 C and thus, limits usage in a high-temperature scenario. Martensitic stainless bearing steels like 440C and BG42 have better corrosion performance, though they need to receive a well-managed heat treatment to balance between hardness, toughness, and corrosion. The higher temperatures of the austenitizing process, together with protective atmospheres, a cryogenic treatment, and low-temperature tempering, allows hardness levels almost equal to non-stainless steels, although usually at compromised toughness or ability to withstand stress corrosion cracking. Nitrogen alloying and special remelting methods used in advanced corrosion-resistant grades like Cronidur 30 overcome a lot of these constraints by providing fine grained microstructures, high cleanliness and outstanding tempering resistance up to about 500°C based on industrial and materials research summarized by Ahrens International and Reddy et al. [167].

In the case of high temperature and aerospace applications, steel like M50, M50NiL and Pyrowear 675 are the ones to be used. M50 has been improved in terms of its higher hot hardness and fatigue strength through molybdenum-carbide strengthening and habitually undergoes deep tempering and stabilization to guarantee dimensional stability at temperatures close to 316 ^{o}C. M50NiL and Pyrowear 675 use case-hardening processes that carburizing or alloy carburizing that forms a hard and wear-resistant martensitic case based on a hard and low-carbon core. They provide a favourable balance of both fatigue strength and corrosivity as well as the capability to withstand high temperatures and are therefore a good fit in aerospace transmission systems and aerospace bearing systems [95, 167]. The surface engineering treatments are essential in cases where additional improvement of the surface durability is needed.

The introduction of a hard diffusion layer by nitriding of the gas, plasma or ion-based results in a minimum amount of distortion and a high degree of indentation resistance, wear, and surface-initiated fatigue. According to Beer [168], conventional hardening of high-speed and high-temperature bearing steels can be followed by nitriding, which results in almost surface-hardness values above 1000 HV and better resistance to damage due to contamination. Table 5 [Appendix] presents the heat treatment characteristics of different steel grades.

Steel cleanliness and microstructural control are significant factors repeatedly draw attention or in Rolling Contact Fatigue (RCF). Secondary remelting techniques, such as ESR, PESR, and VAR can minimize non-metallic inclusions and chemical segregation and decrease subsurface stress concentrations; subsequently increasing an RCF life via the reduction in surface roughness.

Control of retained austenite after cryogenic treatment or staged tempering is another means for improving the dimensional stability and resistance to fatigue by restricting transformation induced stresses in service.

With an increase in tempering temperature to enhance toughness and thermal stability, there is a trade-off loss of peak hardness, implying that selection of tempering schedules should be load-temperature based rather than hardness based alone [164, 165].

The sensitivity of bearing performance to the selection of heat treatment is demonstrated by a couple of experimental experiments. Devgun and Molian [175] demonstrated that laser transformation hardening of AISI 52100 altered the prevailing wear mechanisms through localized microstructural refinement and produced very high surface hardness and excellent sliding wear resistance as compared to traditional quench-and-temper methods.

More recently, it was shown by Fortini et al. [175] that, with careful control of component geometry and quenching conditions, industrial austempering of 100Cr6 and 100CrMo7 bearing rings can be successfully used to achieve bainitic microstructures with unprecedented toughness.

In complementary work to measure the evolution of phase-fraction and predict dimensional changes during aging in bearing steel with bainitic structure, a useful tool to measure the evolution of phase-fraction and predict dimensional changes during aging in bearing steel with bainitic structure was thermoelectric power measurements.

Heat treatment remains a central design variable in bearing engineering because it governs the balance between hardness, toughness, residual stress, and microstructural stability [177]. While AISI 52100 continues to dominate cost-sensitive and well-lubricated applications, advanced bearing steels such as M50, M50NiL, Pyrowear 675, and Cronidur® 30-enabled by optimized heat-treatment and surface-engineering strategies-are indispensable in high-load, high-speed, high-temperature, and corrosive environments [177, 178].

Selection of an appropriate alloy-process combination must therefore be guided by the full-service envelope, including lubrication regime and operating environment, rather than by hardness or nominal composition alone.



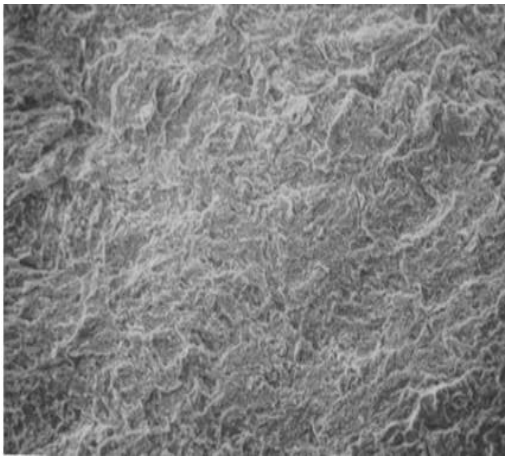

Fig. 11 AISI 52100 typically has grain sizes in the 5-30 µm range after standard heat treatments [179]

Figure 11 presents AISI 52100 typically having grain sizes in the 5-30 µm range after standard heat treatments [179]

This is a review that adds a coherent mechanistic model between abnormal distributions of lubricant-film pressures and wear transitions and rolling contact fatigue in AISI 52100 bearing steel. This work redefines abnormal pressure as a continuum of developing deviations of the classical EHL behaviour and reveals it as the primary cause of surface-initiated cracking, micropitting and scuffing. The review also cites acute experimental and modelling gaps, especially in pure sliding, and gives directions on the way to predictive bearing design.

The findings of this study have direct implications for the design and operation of bearing systems. Improved lubricant selection is made possible by an understanding of the impact of pressure distribution anomalies, especially in applications where maintaining constant film thickness is crucial. The findings further emphasize how crucial it is to regulate operational parameters (such as load and sliding ratio) and

surface roughness to reduce transitions into mixed or border lubrication regimes. This knowledge can be used in predictive maintenance plans, where early lubrication deterioration detection could assist avoid premature bearing failure.

7. Future Research Directions

It is still widely understood that there is a significant knowledge gap between the direct, in-situ observation of the pressure and lubricant film evolution under pure sliding conditions despite the significant progress in Elastohydrodynamic Lubrication (EHL) theory and the characterization of abnormal pressure distributions in bearing steels such as AISI 52100. Most of the existing diagnostic techniques, including traction-curve analysis, infrared thermography, and Spacer Layer Interferometry (SLIM) either infer a redistribution of pressure indirectly, or are typically only useful in regimes dominated by rolling, or in mixed-lubrication regimes. The development of high-resolution, non-invasive imaging and sensing methods capable of capturing transient spikes of pressures, collapse and reformation of films in the presence of sliding dominated contacts would greatly enhance the understanding of the mechanisms of micropitting, scuffing, and surface-initiated cracking. It is also essential that integrated modelling frameworks which explicitly couple contact mechanics, thermal and tribochemistry.

Localized flash temperatures, stress-assisted chemical reactions, and the development or disintegration of protective tribofilms are often associated with abnormal pressure fields. However, chemical film generation and mechanical stress evolution are treated as essentially separate processes in most current models. To forecast wear transitions, fatigue crack initiation, and lubrication failure under less-than-ideal operating conditions, future predictive methods should integrate pressure-driven tribochemical transformations into elastohydrodynamic and finite-element models.

Another intriguing line of inquiry is the use of multiscale modeling techniques. Abnormal pressure distributions often begin at the asperity or debris scale due to surface roughness, third-body entrainment, or local starvation. However, their effects, including rolling contact fatigue and macroscopic spalling, don't show up until millions of cycles at the component size.

1. Researchers could better understand the beginning and development of aberrant wear mechanisms by using hierarchical frameworks that methodically connect nanoscale and microscale contact events to long-term stress accumulation and damage evolution.
2. The lack of statistically sound fatigue and pressure datasets collected under controlled abnormal lubrication conditions is a recurring problem in the literature that makes cross-study comparison, uncertainty quantification, and model validation more difficult.
3. The ability of current frameworks to forecast transient pressure spikes, tribofilm rupture, and fatigue crack initiation under highly non-steady sliding, starved, or thermally distorted conditions is still limited, especially over extended service times, despite significant advancements in elastohydrodynamic and mixed-lubrication modeling.
4. Localized pressure amplification in AISI 52100 bearing steel promotes subsurface stress localization and speeds up crack nucleation under rolling-sliding conditions by interacting strongly with non-metallic inclusions and microstructural heterogeneities.
5. Tribofilm chemistry and pressure stability are also influenced by environmental conditions, such as humidity, oxygen availability, and particulate matter; however, existing experimental interpretations and predictive models do not adequately account for these aspects.

Nonetheless, ensuring that experimental as well as modelling studies are industrially relevant is also important. Abnormal pressure distributions are significant contributors to the efficiency loss, surface distress, and early failure in highly stressed tribological systems, including bearings, gears, and electrical contacts, and not laboratory artifacts. The gap between simplified tribometer experiments and the actual functioning of the components at the component level will require focused research on AISI 52100 that replicates application-relevant sliding-rolling ratios, starvation conditions, thermal gradients and loads spectra. Eventually, it would make high-performance mechanical systems more dependable and long-lived by enabling the translation of lab results into the design-relevant guidelines regarding the choice of lubricants, surface engineering and life prediction.

The mechanisms which are identified in this present study of AISI 52100 bearing steel, but the underlying mechanisms which are found can be generalized to a large group of tribological systems that involve concentrated contacts, such as gears and other rolling-sliding interfaces. It can be generalized to other material systems, the type of lubrication regime, and the operating conditions since the relationship between pressure distribution, lubrication regime and fatigue behaviour is a fundamental property of contact mechanics. Scaling to high-speed or high-temperature applications may however necessitate attention to thermal effects and non-Newtonian behaviour of lubricants.

The next generation of work should be to incorporate the effects of transient lubrication, temperature dependent lubricant behaviour and non-Newtonian fluid models to enhance predictive capability. To further affirm the relationship between pressure anomalies and fatigue onset, controlled experimental studies are necessary to quantitatively

validate the relationship between pressure anomalies and fatigue onset under realistic operating conditions. The integration of real-time monitoring techniques with the proposed framework could also support the development of advanced predictive maintenance systems.

8. Conclusion

The improved predictive capability of the proposed framework lies in its ability to explicitly account for pressure distribution anomalies and their coupling with wear and fatigue processes, which are not simultaneously addressed in conventional approaches. The interaction of lubrication regime, slide-roll ratio, load history, surface roughness, thermal-viscosity effects, and lubricant supply that results in abnormal pressure distributions in lubricated contacts is highlighted in this review. Rather than being isolated anomalies, such pressure behavior is intrinsically multifactorial and is best understood as a spectrum of departures from classical elastohydrodynamic predictions. In bearing steels, these variations result in localized stress concentrations that hasten wear transitions, surface-initiated cracking, and micropitting.

This synthesis's main contribution is to highlight the predictive value of clearly connecting observed wear and fatigue outcomes to abnormal pressure behavior. Conditions that encourage oxidative wear, micropitting, and scuffing in AISI 52100 and related bearing steels can be more accurately identified by combining post-mortem surface characterization, experimental observations, and modelling techniques, such as PVt-based frameworks and Weibull life mapping.

These mappings improve the mechanistic understanding of rolling contact fatigue and offer a useful foundation for life prediction in demanding applications such as high-load electrical contacts, rolling bearings, and gears. This review recognizes the evolution of starvation, shear heating, and pressure amplification over asperity into clear failure modes, and clear mitigation pathways through a design and engineering lens. The most important strategies to stabilize pressure distributions and extend the life of components are to ensure sufficient film parameters ($\xi > 2$), to select the appropriate lubricant viscosity, to improve surface finish, and to ensure reliable lubricant replenishment. A crucial prerequisite for the upcoming generation of bearing steels and lubrication technologies is the creation of integrated multiscale models that integrate contact mechanics with tribochemical processes. Future advancements will require a multimodal strategy that incorporates advanced in-situ diagnostics that can resolve transient pressure evolution, multiscale modelling of stress and tribochemistry, and material-lubricant systems designed to stabilize pressure fields under pure sliding and mixed-contact conditions. A path toward more predictable, dependable, and long-lasting bearing systems under increasingly harsh operating conditions is provided by the implementation of standardized testing procedures that link abnormal pressure patterns to fatigue life, in conjunction with adaptive operational controls and enhanced bearing design strategies.

This review improves our understanding of bearing tribology by integrating lubrication theory, pressure distribution, material reactivity, and fatigue behavior into a unified analytical framework. In addition to providing a clearer mechanistic explanation of bearing deterioration than is typically found in reviews, the proposed synthesis establishes the foundation for additional modeling and experimental study.

Conflicts of Interest

The authors declare that they have no known competing financial interests or personal relationships that could have appeared to influence the work reported in this paper.

Funding Statement

This work is supported by the South African Research Chairs Initiative of the Department of Science and Technology and the National Research Foundation of South Africa (Grant No. PSTD250326306545).

Acknowledgments

National Research Foundation of South Africa is duly acknowledged for this research. Joseph: Writing, review & editing, Writing - original draft; Thywill: Review & editing, Supervision, Funding acquisition, and Enesi: Review and editing.

Data Availability

Data sharing is not applicable to this article as no datasets were generated or analysed during the current study.

Reference

[1] Zobayer Eusufzai, "Impact of Advanced Lubrication Management Systems on Equipment Longevity and Operational Efficiency in Smart Manufacturing Environments," *ASRC Procedia: Global Perspectives in Science and Scholarship*, vol. 1, no. 1, pp. 618-653, 2025. [CrossRef] [Google Scholar] [Publisher Link]

[2] V.V. Karanović et al., "Benefits of Lubricant Oil Analysis for Maintenance Decision Support: A Case Study," *IOP Conference Series: Materials Science and Engineering*, vol. 393, pp. 1-8, 2018. [CrossRef] [Google Scholar] [Publisher Link]

[3] Robert M. Gresham, and George E. Totten, *Lubrication and Maintenance of Industrial Machinery: Best Practices and Reliability*, 1st ed., CRC press, 2009. [Google Scholar] [Publisher Link]

[4] R. David Whitby, *Lubricant Analysis and Condition Monitoring*, 1st ed., CRC Press, 2021. [CrossRef] [Google Scholar] [Publisher Link]

[5] Theo Mang, Kirsten Bobzin, and Thorsten Bartels, *Industrial Tribology: Tribosystems, Friction, Wear and Surface Engineering, Lubrication*, John Wiley and Sons, 2010. [CrossRef] [Google Scholar] [Publisher Link]

[6] Anthony Chukwunonso Opia et al., "A Review on Bio-Lubricants as an Alternative Green Product: Tribological Performance, Mechanism, Challenges and Future Opportunities," *Tribology Online*, vol. 18, no. 2, pp. 18-33, 2023. [CrossRef] [Google Scholar] [Publisher Link]

[7] Andreas Willing, "Lubricants based on Renewable Resources-An Environmentally Compatible Alternative to Mineral Oil Products," *Chemosphere*, vol. 43, no. 1, pp. 89-98, 2001. [CrossRef] [Google Scholar] [Publisher Link]

[8] Zenon Pawlak, *Tribochemistry of Lubricating Oils*, 1st ed., Elsevier, vol. 45, 2003. [Google Scholar] [Publisher Link]

[9] Leslie R. Rudnick, *Synthetics, Mineral Oils, and Bio-based Lubricants: Chemistry and Technology*, 3rd ed., CRC Press, 2020. [CrossRef] [Google Scholar] [Publisher Link]

[10] Joseph V. Koleske, Robert Springate, and Darlene Brezinski, "Additives Handbook," *Paint and Coatings Industry*, vol. 6, pp. 1-64, 2011. [Google Scholar]

[11] Jan C.J. Bart, *Additives in Polymers: Industrial Analysis and Applications*, John Wiley and Sons, 2005. [CrossRef] [Google Scholar] [Publisher Link]

[12] Werner J. Auhorn, "Chemical Additives," *Handbook of Paper and Board*, pp. 62-149, 2006. [CrossRef] [Google Scholar] [Publisher Link]

[13] Zheng Bo et al., "Surface-Dominant Pseudocapacitive Supercapacitors with High Specific Energy and Power for Energy Storage," *Journal of Energy Storage*, vol. 42, pp. 1-11, 2022. [CrossRef] [Google Scholar] [Publisher Link]

[14] Kun Hong Hu et al., "Synthesis of Nano-MoS_2/TiO_2 Composite and its Catalytic Degradation Effect on Methyl Orange," *Journal of Materials Science*, vol. 45, no. 10, pp. 2640-2648, 2010. [CrossRef] [Google Scholar] [Publisher Link]

[15] R. Balaji Natarajan et al., "Advances in Nanomaterials as Lubricant Additives: A Systemic Review," *Surface Review and Letters*, vol. 32, no. 12, 2025. [CrossRef] [Google Scholar] [Publisher Link]

[16] Kevin Gilley, "*Fundamental Interfacial Studies of Advanced Solid Lubricants and their Operating Environments*," University of Florida, vol. 72, 2013. [Google Scholar] [Publisher Link]

[17] Meirong Yi, and Chenhui Zhang, "The Synthesis of MoS_2 Particles with Different Morphologies for Tribological Applications," *Tribology International*, vol. 116, pp. 285-294, 2017. [CrossRef] [Google Scholar] [Publisher Link]

[18] Kun Hong Hu et al., "The Effect of Morphology on the Tribological Properties of MoS2 in Liquid Paraffin," *Tribology Letters*, vol. 40, no. 1, pp. 155-165, 2010. [CrossRef] [Google Scholar] [Publisher Link]

[19] Xianguo Hu, "On the Size Effect of Molybdenum Disulfide Particles on Tribological Performance," *Industrial Lubrication and Tribology*, vol. 57, no. 6, pp. 255-259, 2005. [CrossRef] [Google Scholar] [Publisher Link]

[20] Kunhong Hu et al., "Tribological Properties of MoS_2 Nano-Balls as Filler in Polyoxymethylene-Based Composite Layer of Three-Layer Self-Lubrication Bearing Materials," *Wear*, vol. 266, no. 11-12, pp. 1198-1207, 2009. [CrossRef] [Google Scholar] [Publisher Link]

[21] Wenyang Zhang et al., "Fundamental Understanding of the Tribological and Thermal Behavior of Ag-MoS_2 Nanoparticle-Based Multi-Component Lubricating System," *Wear*, vol. 288, pp. 9-16, 2012. [CrossRef] [Google Scholar] [Publisher Link]

[22] Ziyan Lu et al., "MoS_2 Nanomaterials as Lubricant Additives: A Review," *Lubricants*, vol. 11, no. 12, pp. 1-27, 2023. [CrossRef] [Google Scholar] [Publisher Link]

[23] Lei Chen et al., "Oil-Soluble Sulfur-Containing Organic Molybdenum as Lubricant Additives: A Review," *Journal of Tribology*, vol. 146, no. 12, 2024. [CrossRef] [Google Scholar] [Publisher Link]

[24] Aaron Thornley, "*The Interactions of Surface-Active Engine Oil Additives in Low Viscosity Engine Oils and their Effect on Tribological Performance*," University of Leeds, pp. 1-295, 2023. [Google Scholar] [Publisher Link]

[25] Wei Qi et al., "Molecular Structures, Tribological Properties, and Working Mechanisms of Sulfur-and Phosphorus-Free Organic Molybdenum as additives in Lubricants: A Short Review," *Journal of Tribology*, vol. 146, no. 11, 2024. [CrossRef] [Google Scholar] [Publisher Link]

[26] Xu Cao et al., "Tribological Properties and Synergetic Self-Lubricating Mechanism of PS-PAO based Nanocapsules with MoDTC Additives," *Tribology International*, vol. 186, pp. 1-10, 2023. [CrossRef] [Google Scholar] [Publisher Link]

[27] Deepak Gupta, et al., "Metal-based Nanolubricants: Current and Future Perspectives," *Nanolubricants: Generation and Applications*, pp. 89-133, 2024. [CrossRef] [Google Scholar] [Publisher Link]

[28] Zhengquan Jiang et al., "Two-Dimensional Nanomaterials as Lubricant Additives: The State-of-the-Art and Future Prospects," *Journal of Materials Chemistry C*, vol. 13, no. 9, pp. 4327-4373, 2025. [CrossRef] [Google Scholar] [Publisher Link]

[29] Vladimir An, Yuri Irtegov, and Charles de Izarra, "Study of Tribological Properties of Nanolamellar WS_2 and MoS_2 as Additives to Lubricants," *Journal of Nanomaterials*, vol. 2014, no. 1, pp. 1-8, 2014. [CrossRef] [Google Scholar] [Publisher Link]

[30] Sangita Kumari, Ajay Chouhan, and Om P. Khatri, *Nanostructured Layered Materials as Novel Lubricant Additives for Tribological Applications*, Springer Cham, pp. 157-178, 2020. [CrossRef] [Google Scholar] [Publisher Link]

[31] Shubrajit Bhaumik, and Viorel Paleu, "Wear and Rolling Contact Fatigue Analysis of AISI 52100 Bearing Steel in Presence of Additivated Lubricants," *Metals*, vol. 11, no. 6, pp. 1-17, 2021. [CrossRef] [Google Scholar] [Publisher Link]

[32] M.Z. Saidi et al., "Improved Tribological Properties, Thermal and Colloidal Stability of Poly-α-Olefins based Lubricants with Hydrophobic MoS2 Submicron Additives," *Journal of Colloid and Interface Science*, vol. 562, pp. 91-101, 2020. [CrossRef] [Google Scholar] [Publisher Link]

[33] Ayush Jain, Abhishek Singh, and Arendra Pal Singh, "Effect of Tribological Parameters on Sliding Wear and Friction Coefficient which Relates to Preload Loss in Tapered Roller Bearing," *Industrial Lubrication and Tribology*, vol. 71, no. 1, pp. 61-73, 2019. [CrossRef] [Google Scholar] [Publisher Link]

[34] Gwidon Stachowiak, and Andrew W. Batchelor, *Engineering Tribology*," 3rd ed., Elsevier, 2005. [Google Scholar] [Publisher Link]

[35] Ziwei Li et al., "Cross-Scale Mechanical Contact Analysis from Asperities to Rough Surfaces: A Critical Review," *Coatings*, vol. 15, no. 3, pp. 1-29, 2025. [CrossRef] [Google Scholar] [Publisher Link]

[36] Suhaib Ardah, Francisco J. Profito, and Daniele Dini, "A Comprehensive Review and Trends in Lubrication Modelling," *Advances in Colloid and Interface Science*, vol. 342, pp. 1-33, 2025. [CrossRef] [Google Scholar] [Publisher Link]

[37] Hikmet Bal, "Influence of Lubricant Properties on Elastohydrodynamic Oil Film Thickness in Angular Contact Ball Bearings: A Numerical Investigation," *Applied Mechanics*, vol. 6, no. 3, pp. 1-15, 2025. [CrossRef] [Google Scholar] [Publisher Link]

[38] Keyang Chen et al., "Research Progress of Improving Surface Friction Properties by Surface Texture Technology," *The International Journal of Advanced Manufacturing Technology*, vol. 116, no. 9, pp. 2797-2821, 2021. [CrossRef] [Google Scholar] [Publisher Link]

[39] Salmiah Kasolang et al., "Preliminary Study of Pressure Profile in Hydrodynamic Lubrication Journal Bearing," *Procedia Engineering*, vol. 41, pp. 1743-1749, 2012. [CrossRef] [Google Scholar] [Publisher Link]

[40] Ali Abbaspur et al., "An Analytical Study on Nonlinear Viscoelastic Lubrication in Journal Bearings," *Scientific Reports*, vol. 13, no. 1, pp. 1-22, 2023. [CrossRef] [Google Scholar] [Publisher Link]

[41] Vrushali Y. Bhalerao, and Sanjay S. Lakade, "Comprehensive Review on Improvement in Surface Properties of Bearing Steel," *Materials Today: Proceedings*, vol. 55, pp. 441-446, 2022. [CrossRef] [Google Scholar] [Publisher Link]

[42] Neeraj Kumar, and R.K. Satapathy, "Bearings in Aerospace, Application, Distress, and Life: A Review," *Journal of Failure Analysis and Prevention*, vol. 23, no. 3, pp. 915-947, 2023. [CrossRef] [Google Scholar] [Publisher Link]

[43] Jun Zhou, "*Investigation of Surface Engineering and Monitoring for Reliable Wind Turbine Gearboxes*," University of Birmingham, 2017. [Google Scholar] [Publisher Link]

[44] B.J. Hamrock, and D. Dowson, "Isothermal elastohydrodynamic lubrication of point contacts: Part 1-Theoretical Formulation," *Journal of Tribology*, vol. 98, no. 2, pp. 223-287, 1976. [CrossRef] [Google Scholar] [Publisher Link]

[45] D. Dowson, "Elastohydrodynamic and Micro-Elastohydrodynamic Lubrication," *Wear*, vol. 190, no. 2, pp. 125-138, 1995. [CrossRef] [Google Scholar] [Publisher Link]

[46] R.J. Chittenden et al., "A Theoretical Analysis of the Isothermal Elastohydrodynamic Lubrication of concentrated Contacts. I. Direction of Lubricant Entrainment Coincident with the Major Axis of the Hertzian Contact Ellipse," *Proceedings of the Royal Society of London. A. Mathematical and Physical Sciences*, vol. 397, no. 1813, pp. 245-269, 1985. [Google Scholar] [Publisher Link]

[47] Dong Zhu, and Q. Jane Wang, "Elastohydrodynamic Lubrication: A Gateway to Interfacial Mechanics—Review and Prospect," *Journal of Tribology*, vol. 133, no. 4, 2011. [CrossRef] [Google Scholar] [Publisher Link]

[48] D. Dowson, and Z.M. Jin, "Micro-Elastohydrodynamic Lubrication of Low Elastic Modulus Solids on Rigid Substrates," *Journal of physics D: Applied physics*, vol. 25, 1992. [CrossRef] [Google Scholar] [Publisher Link]

[49] H. Spikes, "The Borderline of Elastohydrodynamic and Boundary Lubrication," *Proceedings of the Institution of Mechanical Engineers, Part C: Journal of Mechanical Engineering Science*, vol. 214, no. 1, pp. 23-37, 2000. [CrossRef] [Google Scholar] [Publisher Link]

[50] Jean-Pierre Chaomleffel, Gérard Dalmaz, and Philippe Vergne, "Experimental Results and Analytical Predictions of EHL Film Thickness," *Tribology International*, vol. 40, no. 10-12, pp. 1543-1552, 2007. [Google Scholar] [Publisher Link]

[51] W. Habchi, S. Bair, and P. Vergne, "On Friction Regimes in Quantitative Elastohydrodynamics," *Tribology International*, vol. 58, pp. 107-117, 2013. [CrossRef] [Google Scholar] [Publisher Link]

[52] Mohammad Lutfar Rahaman et al., "A Review on Frictional Torque Reduction Approaches for Energy Efficient Roller Bearings," *Advances in Mechanical Engineering*, vol. 17, no. 5, pp. 1-22, 2025. [CrossRef] [Google Scholar] [Publisher Link]

[53] Samuel M. Gbashi et al., "From Academic to Industrial Research: A Comparative Review of Advances in Rolling Element Bearings for Wind Turbine Main Shaft," *Engineering Failure Analysis*, vol. 163, pp. 1-23, 2024. [CrossRef] [Google Scholar] [Publisher Link]

[54] Nagaraj K. Arakere, "Gigacycle Rolling Contact Fatigue of Bearing Steels: A Review," *International Journal of Fatigue*, vol. 93, pp. 238-249, 2016. [CrossRef] [Google Scholar] [Publisher Link]

[55] J. Halme, and P. Andersson, "Rolling Contact Fatigue and Wear Fundamentals for Rolling Bearing Diagnostics-State of the Art," *Proceedings of the Institution of Mechanical Engineers, Part J: Journal of Engineering Tribology*, vol. 224, no. 4, pp. 377-393, 2010. [CrossRef] [Google Scholar] [Publisher Link]

[56] A.V. Borgaonkar, and I. Syed, "Effect of Coatings on Rolling Contact Fatigue and Tribological Parameters of Rolling/Sliding Contacts under Dry/Lubricated Conditions: A Review," *Sādhanā*, vol. 45, no. 1, 2020. [CrossRef] [Google Scholar] [Publisher Link]

[57] K. Jalaja et al., "Metallurgical Analysis of Surface Distress on Balls during the Operation of AISI 440C Ball Bearings for Satellite Applications," *Engineering Failure Analysis*, vol. 124, pp. 1-10, 2021. [CrossRef] [Google Scholar] [Publisher Link]

[58] H.V. Squires, and S.J. Radcliffe, "A Comparison of the Performance of AISI 52100 and AISI 440C Ball Bearings in a Corrosive Environment," *Journal of Materials Science*, vol. 18, no. 12, pp. 3611-3620, 1983. [CrossRef] [Google Scholar] [Publisher Link]

[59] E.V. Zaretsky, "Rolling Bearing Steels–A Technical and Historical Perspective," *Materials Science and Technology*, vol. 28, no. 1, pp. 58-69, 2012. [CrossRef] [Google Scholar] [Publisher Link]

[60] Xiaoming Zong, Wenming Jiang, and Zitian Fan, "Characteristics and Wear Performance of Borided AISI 440C Martensitic Stainless Steel," *Materials Express*, vol. 8, no. 6, pp. 500-510, 2018. [Google Scholar]

[61] R. Rejith, "Relating Rolling Contact Fatigue (RCF) Life to the Microstructure Evolution in Aerospace Grade Bearing Steels: A Comparison of Cronidur-30 with AISI 440C," *International Journal of Fatigue*, vol. 186, pp. 1-14, 2024. [CrossRef] [Google Scholar] [Publisher Link]

[62] Ball Bearing Material Options, Rings and Balls, 2017. [Online]. Available: https://schatzbearing.com/ball-bearing-technical-info/material-options/

[63] Grade 440C Martensitic Stainless Steel, AZO Materials, 2016. [Online]. Available: https://www.azom.com/article.aspx?ArticleID=12577

[64] Christopher DellaCorte, and Lewis E. Moore, "Launch Load Resistant Spacecraft Mechanism Bearings Made from Niti Superelastic Intermetallic Materials," *The* 42nd Aerospace Mechanism Symposium, pp. 1-14, 2014. [Google Scholar] [Publisher Link]

[65] Jianlin Sun et al., "Effects of Alloying Elements and Microstructure on Stainless Steel Corrosion: A Review," *Steel Research International*, vol. 93, no. 5, 2022. [CrossRef] [Google Scholar] [Publisher Link]

[66] Francesca Borgioli, "The Corrosion Behavior in Different Environments of Austenitic Stainless Steels Subjected to Thermochemical Surface Treatments at Low Temperatures: An Overview," *Metals*, vol. 13, no. 4, PP. 1-33, 2023. [CrossRef] [Google Scholar] [Publisher Link]

[67] Yuantao Xu et al., "The Effect of Microstructure Evolution on the Mechanical Properties of Martensite Ferritic Steel During Long-Term Aging," *Acta Materialia*, vol. 131, pp. 110-122, 2017. [CrossRef] [Google Scholar] [Publisher Link]

[68] Harish Hirani, *Corrosion, Environmental Degradation, and Surface Engineering: Understanding, Mitigation, and Prevention*, 1st ed., CRC Press, 2025. [Google Scholar] [Publisher Link]

[69] Han Peng et al., "A Review of Research on Wind Turbine Bearings' Failure Analysis and Fault Diagnosis," *Lubricants*, vol. 11, no. 1, pp. 1-33, 2023. [CrossRef] [Google Scholar] [Publisher Link]

[70] He-Fei Li et al., "Fatigue Failure Mechanism of High-Speed Train Bearing Steel After Long-Term Service," *Engineering Failure Analysis*, vol. 165, pp. 1-9, 2024. [CrossRef] [Google Scholar] [Publisher Link]

[71] Bing Su, Chunhao Lu, and Chenghui Li, "Current Status of Research on Hybrid Ceramic Ball Bearings," *Machine*s, vol. 12, no. 8, pp. 1-28, 2024. [CrossRef] [Google Scholar] [Publisher Link]

[72] Vrushali Y. Bhalerao, and Sanjay S. Lakade, "Comprehensive Review on Improvement in Surface Properties of Bearing Steel," *Materials Today: Proceedings*, vol. 55, pp. 441-446, 2022. [CrossRef] [Google Scholar] [Publisher Link]

[73] S.A. Pakhomova, and A.I. Povalyayev, "Silicon Nitride-Based Ceramic Composite Materials for Corrosion-Resistant Rolling Bearings," *IOP Conference Series: Materials Science and Engineering*, vol. 683, no. 1, pp. 1-6, 2019. [CrossRef] [Google Scholar] [Publisher Link]

[74] Luo Yue et al., "Effect of Temperature on the Friction Performance and Mechanisms of Si3N4 and Steel Interfaces in Oil-Lubricated Term Rolling Bearing," *Industrial Lubrication and Tribology*, vol. 77, no. 8, pp. 1360-1369, 2025. [CrossRef] [Google Scholar] [Publisher Link]

[75] Wei-Jian Miao et al., "Additive Manufacturing of Advanced Structural Ceramics for Tribological Applications: Principles, Techniques, Microstructure and Properties," *Lubricants*, vol. 13, no. 3, pp. 1-38, 2025. [CrossRef] [Google Scholar] [Publisher Link]

[76] Riyadh A. Al-Samarai, and Yarub Al-Douri, *Friction and Wear in Metals*, 1st ed., Springer Singapore, 2024. [CrossRef] [Google Scholar] [Publisher Link]

[77] Douglas E. Wolfe et al., "A Comprehensive Review of Modern Engineered Ceramics Coatings for Optimised Resistance to Wear and Corrosion," *Advances in Applied Ceramics, Structural, Functional and Bioceramics*, vol. 122, no. 3-4, pp. 81-100, 2023. [CrossRef] [Google Scholar] [Publisher Link]

[78] Room Town, and Country - Session PL Plenary Lecture, "Morning, April 24, 2018," pp. 1-122, 2017. [Google Scholar]

[79] S. Stewart, R. Ahmed, "Rolling Contact Fatigue of Surface Coatings—A Review," *Wear*, vol. 253, no. 11-12, pp. 1132-1144, 2002. [CrossRef] [Google Scholar] [Publisher Link]

[80] M.R. Ranju, Y. Arivu, and D. Kesavan, "Experimental Studies of Rolling and Rolling-Sliding Contact Fatigue Behaviour of High Nitrogen Alloyed Cronidur-30 Bearing Steel," *Wear*, vol. 574-575, pp. 1-20, 2025. [CrossRef] [Google Scholar] [Publisher Link]

[81] Zhuofan Xia et al., "Rolling Contact Fatigue Failure Mechanism of Bearing Steel on Different Surface Roughness Levels under Heavy Load," *International Journal of Fatigue*, vol. 179, pp. 1-15, 2024. [CrossRef] [Google Scholar] [Publisher Link]

[82] T. Nishimura, "Electrochemical Behaviour and Structure of Rust Formed on Si-and Al-Bearing Steel after Atmospheric Exposure," *Corrosion science*, vol. 52, no. 11, pp. 3609-3614, 2010. [CrossRef] [Google Scholar] [Publisher Link]

[83] Bernhard Elsener et al., "Nickel-Free Manganese Bearing Stainless Steel in Alkaline Media—Electrochemistry and Surface Chemistry," *Electrochimica Acta*, vol. 56, no. 12, pp. 4489-4497, 2011. [CrossRef] [Google Scholar] [Publisher Link]

[84] Nagaraj K. Arakere, "Gigacycle Rolling Contact Fatigue of Bearing Steels: A Review," *International Journal of Fatigue*, vol. 93, pp. 238-249, 2016. [CrossRef] [Google Scholar] [Publisher Link]

[85] Riyadh A. Al-Samarai, and Yarub Al-Douri, *Friction and Wear in Metals*, 1st ed., Springer Singapore, 2024. [CrossRef] [Google Scholar] [Publisher Link]

[86] Giovanni Straffelini, *Materials for Tribology*, Friction and Wear: Methodologies for Design and Control, Springer Cham, 2015. [CrossRef] [Google Scholar] [Publisher Link]

[87] Giovanni Straffelini, and Alberto Molinari, "Mild Sliding Wear of Fe–0.2% C, Ti–6% Al–4% V and Al-7072: A Comparative Study," *Tribology letters*, vol. 41, no. 1, pp. 227-238, 2011. [CrossRef] [Google Scholar] [Publisher Link]

[88] Dominique François, André Pineau, and André Zaoui, *Contact Mechanics; Friction and Wear*, Mechanical Behaviour of Materials, pp. 483-550, 2012. [CrossRef] [Google Scholar] [Publisher Link]

[89] Yinglong Wang, Jorge E. Fernández, and D.G. Cuervo, "Rolling-Contact Fatigue Lives of Steel AISI 52100 Balls with Eight Mineral and Synthetic Lubricants," *Wear*, vol. 196, no. 1-2, pp. 110-119, 1996. [CrossRef] [Google Scholar] [Publisher Link]

[90] Focus on High-End Bearings, CN-SC Bearing, 2026. [Online]. Available: https://www.cn-scbearing.com

[91] Steel Structure, Qingdao Xinguangzheng Steel Structure Co., Ltd., 1997. [Online]. Available: https://www.sinosteelstructure.com/products.html

[92] E.R. Booser, "Bearing Materials," *Kirk-Othmer Encyclopedia of Chemical Technology*, 2000. [CrossRef] [Google Scholar] [Publisher Link]

[93] Miniature Bearings, "Miniature Ball Bearings," *Journal of Scientific Instruments*, vol. 31, no. 3, pp. 113-113, 1954. [CrossRef] [Google Scholar] [Publisher Link]

[94] Armen Kvryan et al., "Electrochemical Corrosion Test Methods for Rapid Assessment of Aerospace Bearing Steel Performance," *11th International Symposium on Rolling Bearing Steels: Progress in Bearing Steel Technologies and Bearing Steel Quality Assurance*. *ASTM International*, pp. 466-486, 2017. [CrossRef] [Google Scholar] [Publisher Link]

[95] Schaeffler Technologies GmbH, *Rolling Bearings in Turbochargers*, Solving the Powertrain Puzzle, pp. 202-210, 2014. [CrossRef] [Google Scholar] [Publisher Link]

[96] FH, Your Reliable Business Partner-FUHONG STEEL, FH, 2022. [Online]. Available: https://www.round-steel.com/alloy-steel/

[97] Carpenter Technology, Pyrowear® 675, Carpenter Technology, 2026. [Online]. Available: https://www.carpentertechnology.com/alloy-finder/pyrowear-675

[98] ASM International, Carpenter A-21 Carburizing Steel Provides Deep Hard Case and Tough Ductile Core, ASM International, 2020. [Online]. Available: https://www.asminternational.org/news/40383418/?u=

[99] European Commission, "*New Generation of Aeronautical Bearings for Extreme Environmental Constraints*," European Commission, 2024. [Online]. Available: https://cordis.europa.eu/project/id/30937/reporting

[100] Sullivan Steel, 2026. [Online]. Available: https://www.sullivansteel.com

[101] Chao Zhao et al., "Investigation of the Corrosion-Wear Interaction Behavior of 8Cr4Mo4V Bearing Steel at Various Corrosion Intervals," *Coatings*, vol. 14, no. 10, pp. 1-16, 2024. [CrossRef] [Google Scholar] [Publisher Link]

[102] Franz-Josef Ebert, "An Overview of Performance Characteristics, Experiences and Trends of Aerospace Engine Bearings Technologies," *Chinese Journal of Aeronautics*, vol. 20, no. 4, pp. 378-384, 2007. [CrossRef] [Google Scholar] [Publisher Link]

[103] James A. Greenwood, "Elastohydrodynamic Lubrication," *Lubricants*, vol. 8, no. 5, pp. 1-30, 2020. [CrossRef] [Google Scholar] [Publisher Link]

[104] George W. Greene et al., "Lubrication and Wear Protection of Natural (Bio) Systems," *Polymer Adhesion, Friction, and Lubrication*, pp. 83-133, 2013. [CrossRef] [Google Scholar] [Publisher Link]

[105] Arnaud Ruellan Du Créhu, "*Tribological Analysis of White Etching Crack (WEC) Failures in Rolling Element Bearings*," Hal Theses, 2014. [CrossRef] [Google Scholar] [Publisher Link]

[106] Thi-Na Ta et al., "Tribological Characteristics and Vibration Response of Grease Lubricated Contacts under Environmental Particles and Water Impact," *Wear*, vol. 550-551, pp. 1-13, 2024. [CrossRef] [Google Scholar] [Publisher Link]

[107] Westin Downtown, "International Joint Tribology Conference," *International Joint Tribology Conference Preliminary Program Guide and Schedule*, pp. 1-77, 2012. [Google Scholar]

[108] Farshid Sadeghi et al., "A Review of Rolling Contact Fatigue," *Journal of Tribology*, vol. 131, no. 4, 2009. [CrossRef] [Google Scholar] [Publisher Link]

[109] Ciro Santus et al., "Surface and Subsurface Rolling Contact Fatigue Characteristic Depths and Proposal of Stress Indexes," *International Journal of Fatigue*, vol. 45, pp. 71-81, 2012. [CrossRef] [Google Scholar] [Publisher Link]
[110] Muhammad U. Abdullah, and Zulfiqar A. Khan, "A Multiscale Overview of Modelling Rolling Cyclic Fatigue in Bearing Elements," *Materials*, vol. 15, no. 17, pp. 1-19, 2022. [CrossRef] [Google Scholar] [Publisher Link]
[111] Gerhard Poll et al., "Starved Lubrication in Rolling Contacts-A Review," *Bearing World*, vol. 4, pp. 69-81, 2019. [Google Scholar]
[112] Yonggang Meng et al., "A Review of Recent Advances in Tribology," *Friction*, vol. 8, no. 2, pp. 221-300, 2020. [CrossRef] [Google Scholar] [Publisher Link]
[113] Huaiju Liu et al., "A Review on Micropitting Studies of Steel Gears," *Coatings*, vol. 9, no. 1, pp. 1-27, 2019. [CrossRef] [Google Scholar] [Publisher Link]
[114] Ruchita Patel et al., "A Review of Mixed Lubrication Modelling and Simulation," *Tribology in Industry*, vol. 44, no. 1, pp. 150-168, 2022. [CrossRef] [Google Scholar] [Publisher Link]
[115] Pieter Martin Lugt, and Guillermo E. Morales-Espejel, "A Review of Elasto-Hydrodynamic Lubrication Theory," *Tribology Transactions*, vol. 54, no. 3, pp. 470-496, 2011. [CrossRef] [Google Scholar] [Publisher Link]
[116] Herbert S. Cheng, "Mixed Lubrication and Lubricated Wear," *Tribology Series*, vol. 25, pp. 181-191, 1993. [CrossRef] [Google Scholar] [Publisher Link]
[117] Guillermo E. Morales-Espejel, "Surface Roughness Effects in Elastohydrodynamic Lubrication: A Review with Contributions," *Proceedings of the Institution of Mechanical Engineers, Part J: Journal of Engineering Tribology*, vol. 228, no. 11, pp. 1217-1242, 2014. [CrossRef] [Google Scholar] [Publisher Link]
[118] A.V. Olver, "The Mechanism of Rolling Contact Fatigue: An Update," *Proceedings of the Institution of Mechanical Engineers, Part J: Journal of Engineering Tribology*, vol. 219, no. 5, pp. 313-330, 2005. [CrossRef] [Google Scholar] [Publisher Link]
[119] R.W. Snidle et al., "Understanding Scuffing and Micropitting of Gears," *Proceedings at NATO Research and Technology Organisation Specialists' Meeting on the Control and Reduction of Wear in Military Platforms*, Williamsburg, USA, vol. 14, pp. 1-18, 2003. [Google Scholar]
[120] B. Wainwright, and A. Kadiric, "Surface Fatigue in Lubricated Contacts: Mapping the Failure Modes of Micropitting versus Macropitting," *International Journal of Fatigue*, vol. 197, pp. 1-13, 2025. [CrossRef] [Google Scholar] [Publisher Link]
[121] Lidia Galda, Jaroslaw Sep, and Slawomir Swirad, "Effect of the Sliding Element Surface Topography on the Oil Film Thickness in EHD Lubrication in Non-Conformal Contact," *Materials*, vol. 15, no. 21, pp. 1-17, 2022. [CrossRef] [Google Scholar] [Publisher Link]
[122] Yonggang Meng et al., "A Review of Advances in Tribology in 2020-2021," *Friction*, vol. 10, no. 10, pp. 1443-1595, 2022. [CrossRef] [Google Scholar] [Publisher Link]
[123] Jože Flašker et al., "Numerical Simulation of Surface Pitting due to Contact Loading," *International Journal of Fatigue*, vol. 23, no. 7, pp. 599-605, 2001. [CrossRef] [Google Scholar] [Publisher Link]
[124] K.S. Chan, and M.P. Enright, "A Probabilistic Micromechanical Code for Predicting Fatigue Life Variability: Model Development and Application," *Journal of Engineering for Gas Turbines and Power*, vol. 128, no. 4, pp. 889-895, 2006. [CrossRef] [Google Scholar] [Publisher Link]
[125] Lennie Abdullah et al., "Fatigue Reliability Characterisation of Effective Strain Damage Model using Extreme Value Distribution for Road Load Conditions," *Materials*, vol. 16, no. 1, pp. 1-22, 2023. [CrossRef] [Google Scholar] [Publisher Link]
[126] Tomoyuki Fujii et al., "Influence of Strain Gradient on Fatigue Life of Carbon Steel for Pressure Vessels in Low-Cycle and High-Cycle Fatigue Regimes," *Materials*, vol. 15, no. 2, pp. 1-15, 2022. [CrossRef] [Google Scholar] [Publisher Link]
[127] Luís Coelho et al., "Rolling and Rolling-Sliding Contact Fatigue Failure Mechanisms in 32 CrMoV 13 Nitrided Steel-an Experimental Study," *Applied Sciences*, vol. 11, no. 21, pp. 1-14, 2021. [CrossRef] [Google Scholar] [Publisher Link]
[128] Jun Zhao et al., "An Investigation on the Tribological Properties of Multilayer Graphene and MoS2 Nanosheets as Additives used in Hydraulic Applications," *Tribology International*, vol. 97, pp. 14-20, 2016. [CrossRef] [Google Scholar] [Publisher Link]
[129] Naofumi Hiraoka, and Eiro Yamane, "A Study on the Mechanism of Generating Wear Track Grooves," *Tribology Letters*, vol. 41, no. 3, pp. 479-484, 2011. [CrossRef] [Google Scholar] [Publisher Link]
[130] Quanshun Luo, and Jingzhi Zhu, "Wear Property and Wear Mechanisms of High-Manganese Austenitic Hadfield Steel in Dry Reciprocal Sliding," *Lubricants*, vol. 10, no. 3, pp. 1-18, 2022. [CrossRef] [Google Scholar] [Publisher Link]
[131] Franklin Paz-Triviño, Robison Buitrago-Sierra, and Juan Felipe Santa-Marín, "Wear Resistance and Hardness of Nanostructured Hardfacing Coatings," *Dyna*, vol. 87, no. 214, pp. 146-154, 2020. [Google Scholar]
[132] V. Podgursky et al., "Rippling on Wear Scar Surfaces of Nanocrystalline Diamond Films after Reciprocating Sliding against Ceramic Balls," *Tribology Letters*, vol. 55, no. 3, pp. 493-501, 2014. [CrossRef] [Google Scholar] [Publisher Link]
[133] Long Wang et al., "High Temperature Wear Behaviors of TiAl–TiB_2 Composites," *Tribology Letters*, vol. 65, no. 4, pp. 1-11, 2017. [CrossRef] [Google Scholar] [Publisher Link]
[134] A.A. El-Sayed et al., "Friction and Wear Properties of Polymeric Composite Materials for Bearing Applications," *Wear*, vol. 184, no. 1, pp. 45-53, 1995. [CrossRef] [Google Scholar] [Publisher Link]

[135] Peter J. Blau, "On the Nature of Running-in," *Tribology International*, vol. 38, vol. 11-12, pp. 1007-1012, 2005. [CrossRef] [Google Scholar] [Publisher Link]
[136] Yelong Xiao et al., "Mechanical and Tribological Behaviors of Copper Metal Matrix Composites for Brake Pads used in High-Speed Trains," *Tribology International*, vol. 119, pp. 585-592, 2018. [CrossRef] [Google Scholar] [Publisher Link]
[137] Quanshun Luo et al., "Sliding Wear of Medium-Carbon Bainitic/Martensitic/Austenitic Steel Treated by Short-Term Low-Temperature Austempering," *Wear*, vol. 476, pp. 1-11, 2021. [CrossRef] [Google Scholar] [Publisher Link]
[138] Paweł J. Romanowicz, and Bogdan Szybiński, "Fatigue Life Assessment of Rolling Bearings made from AISI 52100 Bearing Steel," *Materials*, vol. 12, no. 3, pp. 1-23, 2019. [CrossRef] [Google Scholar] [Publisher Link]
[139] Jiri Krupka et al., "Elastohydrodynamic Lubrication of Compliant Circular Contacts near Glass-Transition Temperature," *Lubricants*, vol. 10, no. 7, pp. 1-18, 2022. [CrossRef] [Google Scholar] [Publisher Link]
[140] Dan Holdmeyer, "The Stribeck Curve," *Tribology and Lubrication Technology*, vol. 78, no. 7, pp. 24-25, 2022. [Google Scholar]
[141] Jizhan Wu et al., "Development and Application of High Strength Gears," *The International Journal of Advanced Manufacturing Technology*, vol. 132, no. 7, pp. 3123-3148, 2024. [CrossRef] [Google Scholar] [Publisher Link]
[142] Veniamin Goldfarb, Evgenii Trubachev, and Natalya Barmina, *Advanced Gear Engineering*, Springer Cham, 2018. [CrossRef] [Google Scholar] [Publisher Link]
[143] Kapil Gupta, Neelesh Kumar Jain, and Rudolph Laubscher, *Advanced Gear Manufacturing and Finishing*, Academic Press, 2017. [Google Scholar] [Publisher Link]
[144] Konstantinos D. Bakoglidis, "*Low-Friction and Wear-Resistant Carbon Nitride Coatings for Bearing Components Grown by Magnetron Sputtering*," Dissertations and Theses, Linkopings Universitet, Sweden, 2016. [Google Scholar]
[145] ASTM 52100 Bearing Steel, Otai Special Steel, 2015. [Online]. Available: https://www.astmsteel.com/product/52100-bearing-steel-aisi/
[146] Rambo Yang, Unveiling the Superiority of 52100 Bearing Steel: Understanding the Basics, Linkedin, 2024. [Online]. Available: https://www.linkedin.com/pulse/unveiling-superiority-52100-bearing-steel-basics-rambo-yeung-r65gc
[147] J.M. Beswick, "The Effect of Chromium in High Carbon Bearing Steels," *Metallurgical Transactions A*, vol. 18, no. 11, pp. 1897-1906, 1987. [CrossRef] [Google Scholar] [Publisher Link]
[148] Juan Guillermo Zapata Tamayo et al., "Micropitting Performance and Friction Behaviour of DLC Coated Bearing Steel Surfaces: On the Influence of Glycerol-based Lubricants," *Tribology International*, 196, pp. 1-20, 2024. [CrossRef] [Google Scholar] [Publisher Link]
[149] Pawel Rycerz, and Amir Kadiric, "The Influence of Slide-Roll Ratio on the Extent of Micropitting Damage in Rolling-Sliding Contacts Pertinent to Gear Applications," *Tribology Letters*, vol. 67, no. 2, pp. 1-20, 2019. [CrossRef] [Google Scholar] [Publisher Link]
[150] Aleks Vrček, "*Micro-Pitting and Wear Characterization for Crankshaft Roller Bearing Application*," Doctoral Dissertation, Luleå University of Technology, 2018. [Google Scholar]
[151] M.F. AL-Mayali et al., "Experimental and Numerical Study of Micropitting Initiation in Real Rough Surfaces in a Micro-Elastohydrodynamic Lubrication Regime," *Tribology letters*, vol. 66, no. 4, pp. 1-14, 2018. [CrossRef] [Google Scholar] [Publisher Link]
[152] Siavash Soltanahmadi, "*Tribochemical Investigation of Micropitting in Rolling-Element Bearing Applications: The Influence of Lubricant Additives and Water Contamination*," Ph.D. Thesis, University of Leeds, 2017. [Google Scholar] [Publisher Link]
[153] Lisa-Marie Weniger et al., "Quantifying Hydrogen Concentrations and their Influence on Surface-Initiated Damage in Rolling/Sliding Contacts of 100 Cr6 Bearing Steel," *Tribology Letters*, vol. 73, no. 2, pp. 1-18, 2025. [CrossRef] [Google Scholar] [Publisher Link]
[154] Matti Savolainen, "*An Investigation into Scuffing and Subsurface Fatigue in a Lubricated Rolling/Sliding Contact*," Doctoral Dissertation, Tampere University Dissertations, vol. 57, 2019. [Google Scholar] [Publisher Link]
[155] Simona Dahdah, "*Scuffing Initiation Prediction in a Lubricated Piston Ring Cylinder Liner Contact*," Doctoral Dissertation, Université de Lyon, 2022. [Google Scholar] [Publisher Link]
[156] Serigne Ndiaga Ndiaye, "*Ultimate Behavior of Confined Fluids under Very High Pressure and Shear Stress*," Doctoral Dissertation, Université de Lyon, 2017. [Google Scholar] [Publisher Link]
[157] Ramsey Gohar, *Elastohydrodynamics*, 2nd ed., World Scientific Connect, 2001. [Google Scholar] [Publisher Link]
[158] Piyush Patil, "*Influence of Plastic Anisotropy on the Deformation Behaviour of Austenitic Stainless-Steel during Single Micro-Asperity Wear*," Doctoral Dissertation, Ruhr-Uiversität-Bochu, 2023. [Google Scholar]
[159] Jasim Hasan Ilik AL-Bedhany, "*Effect of Compression, Impact and Slipping on Rolling Contact Fatigue and Subsurface Microstructural Damage*," Doctoral Dissertation, University of Sheffield, 2020. [Google Scholar]
[160] Hao Fu et al., "Experimental Study and Mechanism Analysis of the Influence of Micro-Dimple Geometry on the Adhesion Strength of Textured Coatings," *Coatings*, vol. 14, no. 8, pp. 1-15, 2024. [CrossRef] [Google Scholar] [Publisher Link]
[161] Sufen Dong et al., "Incorporating Super-Fine Stainless Wires to Control Thermal Cracking of Concrete Structures caused by Heat of Hydration," *Construction and Building Materials*, vol. 271, pp. 1-14, 2021. [CrossRef] [Google Scholar] [Publisher Link]

[162] Bowen Liu et al., "Failure Mechanism of Hot Dry Rock under the Coupling Effect of Thermal Cycling and Direct Shear Loading Path," *International Journal of Rock Mechanics and Mining Sciences*, vol. 176, pp. 1-15, 2024. [CrossRef] [Google Scholar] [Publisher Link]

[163] Ekta Yadav, and V.K. Chawla, "An Explicit Literature Review on Bearing Materials and their Defect Detection Techniques," *Materials Today: Proceedings*, vol. 50, pp. 1637-1643, 2022. [CrossRef] [Google Scholar] [Publisher Link]

[164] Yong Su et al., "Effect of Deep Tempering on Microstructure and Hardness of Carburized M50NiL Steel," *Journal of Materials Research and Technology*, vol. 14, pp. 1080-1088, 2021. [CrossRef] [Google Scholar] [Publisher Link]

[165] Zhuan Zhao et al., "Wear Resistance of Cronidur 30 Steel Enhanced by Optimizing the Strengthened Grinding Process (SGP) Parameters using a Box-Behnken Design (BBD) Method," *Journal of Manufacturing Processes*, vol. 122, pp. 7-20, 2024. [CrossRef] [Google Scholar] [Publisher Link]

[166] T. Blass, M. Dinkel, and W. Trojahn, "Bearing Performance as a Function of Structure and Heat Treatment," *Materials Science and Technology*, vol. 32, no. 11, pp. 1079-1085, 2016. [CrossRef] [Google Scholar] [Publisher Link]

[167] C. Anil Kumar Reddy, Nageswara Rao Boggarapu, and T. Srinivasan, "A Review on Heat Treated Bearing Steels for Aerospace Applications," *Materials Today: Proceedings*, vol. 68, pp. 2038-2040, 2022. [CrossRef] [Google Scholar] [Publisher Link]

[168] O. Beer, "Heat Treatment and Properties of High-Temperature Steels for Rolling Bearings," *HTM Journal of Heat Treatment and Materials*, vol. 76, no. 2, pp. 155-171, 2021. [CrossRef] [Google Scholar] [Publisher Link]

[169] Carbide Types in Knife Steels, Knife Steels Nerds, 2019. [Online]. Available: https://knifesteelnerds.com/2019/07/15/carbide-types-in-knife-steels/

[170] I.R. Sare, James I. Mardel, and Anita J. Hill, "Wear-Resistant Metallic and Elastomeric Materials in the Mining and Mineral Processing Industries-An Overview," *Wear*, vol. 250, no. 1-12, pp. 1-10, 2001. [CrossRef] [Google Scholar] [Publisher Link]

[171] Martensitic Stainless Steel, FM Carbide, 2026. [Online]. Available: https://fmcarbide.com/pages/martensitic-stainless-steel

[172] Shengfu Yuan et al., "Evolution of Microstructure and the Influence of Carbides on Hardness Properties in Martensitic Stainless Steel 90Cr18MoV during Heat Treatment," *Metals*, vol. 15, no. 9, pp. 1-17, 2025. [CrossRef] [Google Scholar] [Publisher Link]

[173] FAG OEM und Handel AG, Rolling Bearings Made of Cronidur 30®, FAG OEM und Handel AG, 1999. [Online]. Available: https://www.ahrinternational.com/PDF_catalogues/FAG/WL%2051133E_CRONIDUR30.PDF

[174] M.S. Devgun, and Palaniappa A. Molian, "Experimental Study of Laser Heat-Treated Bearing Steel," *Journal of Materials Processing Technology*, vol. 23, no. 1, pp. 41-54, 1990. [CrossRef] [Google Scholar] [Publisher Link]

[175] Annalisa Fortini et al., "Heat Treatment of Bearing Steels: An Industrial Investigation," *La Metallurgia Italiana*, vol. 114, no. 10, pp. 28-36, 2023. [Google Scholar] [Publisher Link]

[176] E. Tonicello et al., "Rolling Bearing Applications: Some Trends in Materials and Heat Treatments," *Materials Science and Technology*, vol. 28, no. 1, pp. 23-26, 2012. [CrossRef] [Google Scholar] [Publisher Link]

[177] Yongjie Cheng et al., "Research Status of the Influence of Machining Processes and Surface Modification Technology on the Surface Integrity of Bearing Steel Materials," *The International Journal of Advanced Manufacturing Technology*, vol. 125, no. 7, pp. 2897-2923, 2023. [CrossRef] [Google Scholar] [Publisher Link]

[178] Lewis Rosado et al., "Rolling Contact Fatigue Life and Spall Propagation of AISI M50, M50NiL, and AISI 52100, Part I: Experimental Results," *Tribology Transactions*, vol. 53, no. 1, pp. 29-41, 2009. [CrossRef] [Google Scholar] [Publisher Link]

[179] Robby Mannens et al., "Surface Integrity of AISI 52100 Bearing Steel after Robot-based Machine Hammer Peening," *Journal of Manufacturing and Materials Processing*, vol. 4, no. 2, pp. 1-17, 2020. [CrossRef] [Google Scholar] [Publisher Link]

Appendix 1

List of Acronyms

AISI - American Iron and Steel Institute
EHL - Elastohydrodynamic Lubrication
EHD - Elastohydrodynamic
RCF - Rolling Contact Fatigue
SRR - Slide-to-Roll Ratio
λ (Lambda) - Film Parameter (ratio of minimum lubricant film thickness to composite surface roughness)
ESR - Electroslag Remelting
PESR - Pressure Electroslag Remelting
VAR - Vacuum Arc Remelting
VIM - Vacuum Induction Melting
HRC - Rockwell Hardness C Scale
Ra - Arithmetic Mean Surface Roughness
σ - Composite Surface Roughness
h_{min} - Minimum Lubricant Film Thickness
h□ - Central Lubricant Film Thickness
FEA - Finite Element Analysis
E.P. - Extreme Pressure (additive)
ZDDP - Zinc Dialkyldithiophosphate
MoS_2 - Molybdenum Disulfide
WS_2 - Tungsten Disulfide
HYVIS - High-Viscosity Synthetic Polybutene (trade designation)
EHL-RCF - Elastohydrodynamic Lubrication-Rolling Contact Fatigue (coupled behavior)
EHL-TEHD - Thermal Elastohydrodynamic Lubrication
WEC - White Etching Cracks
VIM-VAR - Vacuum Induction Melting followed by Vacuum Arc Remelting
TEHD - Thermo-Elastohydrodynamic
EHDL - Elastohydrodynamic Lubrication
RBE - Rolling Bearing Element
AFM - Atomic Force Microscopy
SEM - Scanning Electron Microscopy
EDS - Energy-Dispersive X-ray Spectroscopy

Appendix

Table 1. Summary of reported experimental designs and operating conditions for AISI 52100 steel

S/N	Reference	Test Configuration	Material & Surface Condition	Lubricant Type / Condition	Operating Conditions	Measured Parameters	Data Acquisition / Repetition
1	Wang et al. [89]	Multi-ball RCF test	AISI 52100 (hardened, polished)	Mineral (additive) oils	Controlled contact pressure (P_o), rolling/sliding	Fatigue life (RCF), crack initiation	Multiple runs; fatigue life averaged (L_{10} basis)
2	Bhaumik et al. [31]	Ball-on-disc (pin-on-disc)	AISI 52100 (ground surface)	Base oil vs WS_2 additive	Sliding contact, varying load and speed	Wear scar, friction coefficient, surface damage	Repeated trials: SEM used for wear characterization
3	Poll et al. [111]	Rolling contact (starvation studies)	Bearing steel (AISI 52100 representative)	Starved lubrication	Reduced inlet supply, variable SRR	Film thickness, micropitting tendency	Experimental and model validation; trends reported
4	Morales-Espejel [117]	EHL (micro-EHL studies)	Smooth vs rough surfaces	Full film to mixed lubrication	Roughness variation, load variation	Pressure distribution, film thickness	Model: experiment comparison; sensitivity analysis
5	Liu et al. [113]	Gear / bearing contact tests	AISI 52100 and similar steels	Mixed lubrication	Cyclic loading, rolling/sliding	Micropitting density, crack initiation	Multiple cycles; statistical trend analysis
6	Patel et al. [114]	Mixed lubrication experiments	Bearing steels	Boundary/ mixed lubrication	Load and speed variation	Friction, wear rate, contact transitions	Experimental and modelling correlation
7	Romanowicz [138]	Fatigue life evaluation	AISI 52100 bearings	Lubricated contact	Variable stress and residual stress states	L_{10} life, failure probability	Weibull statistical analysis
8	Krupka et al. [139]	Roughness: film interaction	AISI 52100 (controlled roughness)	Thin film lubrication	Surface topography variation	Film breakdown zones, pressure spikes	Optical interferometry; repeated measurements
9	Abdullah & Khan [110]	Multiscale RCF modelling and experiments	AISI 52100	Lubricated contact	Cyclic loading, microstructure evolution	Crack initiation, subsurface damage	Model validated with experimental observations

Table 2. Various Steel grades, key properties and applications

Steel / Grade	C (%)	Cr (%)	Other Key Alloying Elements	Key Properties	Typical Applications
SAE 52100 (also, 100Cr6 / SUJ2 / GCr15)	0.95 - 1.10 [93]	1.30-1.60 [93]	Si (0.15-0.35), Mn (0.25-0.45), low P and S, trace Mo/Ni/Cu depending on spec [94]	Through-hardening, high hardness (64 HRC), excellent wear resistance, good contact-fatigue strength, good workability.	Baseline for general-purpose bearings (rings, balls, rollers) where high hardness, load capacity, and fatigue strength are needed; common in automotive, industrial, machinery [95-96].
M50	0.80-0.88(nominal) (Metal Zenith)	4.0-4.5 (Cr) (Metal Zenith) [97]	Mo and often other carbide-forming elements depending on alloy variant. [98]	Better high-temperature strength and hardness retention compared to SAE 52100; suitable for elevated-temperature bearing service; high wear resistance in high-stress	Bearings in aerospace, turbine engines, high-speed spindles, and other applications with elevated temperature or continuous high stress. [98]

				environment. [98]	
M50 NiL (low-noise / carburizing variant of M50)	Lower carbon (carburizing steel) not fixed high-C like SAE 52100; exact C depends on heat-treatment/carburizing spec [98]	High alloy content (Cr, Mo, others depending on alloy recipe) typical alloying adapted for carburizing and high performance [98]	Designed for casehardening to provide a hard surface with a tough ductile core. [98]	Good fatigue strength, good wear resistance, more stable under lubrication-starved or dynamic-load environments; acceptable toughness. [99]	Aerospace and industrial bearings (especially where noise reduction, surface hardness, and fatigue life under mixed or boundary lubrication are needed) [98]
Pyrowear 675 (also "P675")	0.07 (nominal) low carbon carburizing steel. [100]	13.0 (Cr) [100]	Ni2.6%, Co5.4%, Mo1.8%, Mn0.65%, V0.60%, Si0.40% [100]	Carburizable stainless-type bearing steel: after carburizing and heat treatment, obtains high surface hardness (> 60 HRC) plus a tough, ductile core. Good corrosion resistance (case like 440C) and good hot-hardness capability. [100]	Bearings, gears, shafts, and structural components in harsh environments e.g. aerospace, energy, industrial, and transportation applications requiring hard, wear-resistant, corrosion-resistant surfaces with tough cores. [100]
CSS-42L	Case-carburizable / stainless bearing steel nominal composition includes 14.0 % Cr, plus Mo, V, Co (and others) according to specification. [101]	14.0 % Cr (nominal) (ASM International)	Alloying with elements such as Mo, V, Co to balance high strength, wear resistance, corrosion resistance, and core toughness. [101]	Designed to offer a combination of high fracture toughness, corrosion resistance, hot hardness, and wear resistance with a ductile core. [101]	High-temperature and corrosion-critical bearing and gear applications aerospace bearings, high-performance gearboxes, industrial mechanisms under harsh conditions. [102]
Cronidur 30 (also written Cronidur30) / CREN nitrogen-Alloyed Bearing steel	Low carbon, nitrogen-alloyed (exact C low; typical high-nitrogen bearing steel) e.g. per spec: C0.28-0.34 %, N0.35-0.44 % (nitrogen content) [103]	14.5-16.0 % Cr (nominal) [103]	Alloyed with Mo (0.95-1.10 %), possibly V, and high N for corrosion-resistance and high fatigue life. [103]	Very good corrosion resistance (better than many standard bearing steels), good fatigue endurance under lubrication, good scuffing resistance, good dimensional stability; suitable for aerospace and hostile environment bearings. [104-106]	Bearings, ball- and roller-screws, spindles, aerospace and chemical/marine exposed bearings, where corrosion resistance and fatigue life are critical [98].
XD15NW (often as alternative	C0.37-0.45 % (nominal, depending on spec) [103]	Cr15.0-16.5 % nominal [103]	Mo 1.5-1.9 %, V 0.20-0.40 %, N 0.16-0.25 %,	High nitrogen martensitic steel with good hardness (58-60 HRC after heat	Bearings, spindles, aerospace applications, chemical / corrosive / high-stress environments

to Cronidur 30)			other possible alloying depending on spec. [103]	treatment), high fatigue strength, good corrosion resistance considered a viable alternative to Cronidur 30 for aerospace/high-demand bearings. [103]	where standard bearing steels may fail. [103]

Table 3. Data synthesis of pressure anomalies, lubrication behaviour, and fatigue-wear response in AISI 52100

S/N	Reference	Test / Focus	Lubrication Regime / Condition	Pressure / Film Signature	Fatigue / Wear Outcome	Key Insight / Mechanistic Interpretation
1	Wang et al. [89]	RCF and multi-ball tests on AISI 52100	EHL: Mixed (additive-dependent)	Reduced film thickness; increased traction leading to local pressure spikes	Early crack initiation and spalling under poor lubrication	Film degradation directly elevates contact stress, accelerating subsurface fatigue
2	Bhaumik et al. [31]	Additive vs non-additive lubrication	Mixed lubrication	Asperity-dominated contact in base oil; improved film with WS_2	Reduced cracking with additives; micropitting persists under severe conditions	Additives mitigate but do not eliminate pressure-induced fatigue under high load
3	Poll et al. [111]	Starved lubrication (review)	Starved / Mixed	Film collapse; asymmetric pressure distribution; inlet starvation	Micropitting and surface distress; scuffing at high SRR	Lubricant starvation redistributes pressure, promoting surface-driven failure
4	Morales-Espejel [117]	Roughness effects in EHL	Mixed / Micro-EHL	Multi-peak pressure spikes due to roughness	Accelerated micropitting and wear transition	Surface roughness acts as a local stress amplifier under thin film conditions
5	Liu et al. [119]	Micropitting review	Mixed lubrication	Local stress concentration from asperity contacts	Surface crack initiation → micropits → macropitting	Micropitting is a direct consequence of repeated pressure fluctuations at asperities
6	Patel et al. [114]	Mixed lubrication modelling	Mixed regime	Non-Hertzian pressure distribution due to asperity interaction	Increased surface crack density and wear	Transition thresholds governed by film breakdown and asperity load sharing
7	Romanowicz [138]	Fatigue life modelling	EHL resulting in Non-ideal pressure	Modified subsurface stress fields due to traction and residual stress	Reduced L_{10} life; early failure probability increases	Non-uniform pressure fields significantly reduce fatigue life reliability
8	Krupka et al. [139]	Roughness-film interaction	Mixed / Boundary	Local film rupture at asperities; pressure concentration zones	Micropitting and rapid wear progression	Film rupture zones act as initiation sites for damage accumulation
9	Abdullah & Khan [110]	Multiscale RCF modelling	Mixed / Evolving contact	Microstructural evolution amplifies local stress concentration	Subsurface damage and spalling in high-pressure regions	Coupling between material microstructure and pressure anomalies governs fatigue evolution

Table 4. Lubrication regimes and corresponding pressure and failure characteristics

Condition	Friction	Film Regime	Failure Mode	Pressure behaviour
Ideal EHL	Approx. 0.02	Full film	Subsurface fatigue	Smooth (Hertzian-like)
Mixed regime	medium	Partial film	Micropitting	Local spikes
Boundary	High	No film	Severe wear/scuffing	Severe contact

Table 5. Heat treatment characteristics of different steel grades

Grade	Typical austenitize	Quench	Tempering	Specialist steps / notes	Main microstructural / property outcome
SAE 52100 / 100Cr6	820-860 °C	Oil quench (often with agitation)	Temper 150-300°C (single/multiple) to target HRC 58-64	Cryogenic treatment is sometimes used to reduce retained austenite; normalization to refine grains.	Through-hardened martensite and fine carbides yielding high contact fatigue & wear resistance [177, 178]
440C (martensitic stainless)	1040-1080 °C	Oil or air quench (protective pack)	Temper low (100-300 °C) for high HRC (57-61)	Cryogenic cycles are commonly used; protective atmospheres to avoid surface oxidation	High-hardness martensite with secondary carbides yielding best stainless hardness but tempering trades toughness/corrosion resistance [179, 180]
M50 / M50NiL	1000-1065°C (depends on spec)	Oil quench / controlled quench	Multiple tempering cycles (e.g., 400-500 °C stabilization)	Deep tempering / cryo sequences and vacuum processing often applied	Tempered martensite with stable carbides yielding superior hot-hardness, wear & RCF at elevated temps [181].
Pyrowear 675 (P675)	Carburize cycle (low-C core steels require carburizing)	Quench after carburizing (oil/water depending on cycle)	Tempering to balance case hardness / core toughness	Proprietary stainless-carburizing route; delivers hard case and corrosion resistance	Hardened, carburized case (≥60 HRC possible) and tough core. Ideal when surface wear and corrosion needed [98]
Cronidur®30 (high-N, remelted)	Manufacturer-specified; tailored for fine grain and tempering resistance	Quench (process controlled for minimal distortion)	Tempering to give stability up to 500°C	Produced via special remelting (PESR/ESR) to maximize cleanliness; high tempering resistance	Fine martensite with distributed hard phases yielding high fatigue life, corrosion resistance and dimensional stability [182, 183].
Nitriding / Case processes	Pre-treat (cleaning, possible preheat)	N/A (diffusion)	Low-temperature aging / finish	Gas, plasma or ion nitriding; controlled to form hard nitride case without quench distortion	Hard, wear-resistant diffusion case with ductile core. Good for lower distortion than carburizing/quench [98]